Molecular Biology of the Cell
Vol. 14, 871–888, March 2003

Roles of NUDE and NUDF Proteins of *Aspergillus nidulans*: Insights from Intracellular Localization and Overexpression Effects[V]

Vladimir P. Efimov*

Department of Pharmacology, University of Medicine and Dentistry of New Jersey, Robert Wood Johnson Medical School, Piscataway, New Jersey 08854

Submitted June 25, 2002; Revised September 30, 2002; Accepted November 18, 2002
Monitoring Editor: Lawrence S. Goldstein

The NUDF protein of the filamentous fungus *Aspergillus nidulans* functions in the cytoplasmic dynein pathway. It binds several proteins, including the NUDE protein. Green fluorescent protein-tagged NUDF and NUDA (dynein heavy chain) localize to linearly moving dashes ("comets") that coincide with microtubule ends. Herein, deletion of the *nudE* gene did not eliminate the comets of NUDF and NUDA, but affected the behavior of NUDA. Comets were also observed with the green fluorescent protein-tagged NUDE and its nonfunctional C-terminal domain. In addition, overexpressed NUDA and NUDE accumulated in specks that were either immobile or bounced randomly. Neither comets nor specks were observed with the functional N-terminal domain of NUDE, indicating that these structures are not essential for NUDE function. Furthermore, NUDF overproduction totally suppressed deletion of the *nudE* gene. This implies that the function of NUDE is secondary to that of NUDF. Unexpectedly, NUDF overproduction inhibited one conditional *nudA* mutant and all tested *apsA* mutants. An allele-specific interaction between the *nudF* and *nudA* genes is consistent with a direct interaction between NUDF and dynein heavy chain. Because APSA and its yeast homolog Num1p are cortical proteins, an interaction between the *nudF* and *apsA* genes suggests a role for NUDF at the cell cortex.

INTRODUCTION

Cytoplasmic dynein is a multisubunit protein complex that functions as a minus-end–directed microtubule motor. Acting with another complex, dynactin, it powers movement and positioning of diverse cellular organelles in eukaryotic cells. Genetic screens in filamentous fungi *Aspergillus nidulans* and *Neurospora crassa* and in yeast *Saccharomyces cerevisiae* have identified many genes in the cytoplasmic dynein/dynactin pathway (Osmani *et al.*, 1990; Plamann *et al.*, 1994; Robb *et al.*, 1995; Xiang *et al.*, 1994, 1995a; Bruno *et al.*, 1996; Tinsley *et al.*, 1996; Geiser *et al.*, 1997; Vierula and Mais, 1997; Beckwith *et al.*, 1998; Minke *et al.*, 1999; Xiang *et al.*, 1999; Efimov and Morris, 2000; Lee *et al.*, 2001; Zhang *et al.*, 2002). In *A. nidulans*, mutations in dynein and dynactin genes impair distribution of nuclei along hyphae (filamentous fungal cells), which are multinucleated. Because of such phenotypes, the genes are called *nud* (*nu*clear *d*istribution) genes. Dynein/dynactin null mutants are viable, but form abnormally compact colonies and fail to produce conidia (asexual spores). Cytoplasmic microtubules are less dynamic in *nud* mutants (Han *et al.*, 2001), and their destabilization suppresses nuclear distribution defects (Willins *et al.*, 1995; Alberti-Segui *et al.*, 2001). Defects in vesicle trafficking and vacuole distribution are also likely, because they were observed in *N. crassa* dynein/dynactin mutants (Seiler *et al.*, 1999; Lee *et al.*, 2001) and in a dynactin mutant of *Aspergillus oryzae* (Maruyama *et al.*, 2002). In addition to the subunits of dynein and dynactin, genetic screens in the above-mentioned fungi also identified several proteins that do not seem to be components of purified dynein or dynactin complexes, and thus whose relation to dynein/dynactin is not obvious. This work concerns two such proteins of *A. nidulans*, NUDF (Pac1p in *S. cerevisiae*) and NUDE (RO11 in *N. crassa*), encoded by the *nudF* and *nudE* genes, respectively.

According to genetic data, the *nudF* gene of *A. nidulans* and its *S. cerevisiae* homolog Pac1p function in the dynein/dynactin pathway (Xiang *et al.*, 1995a; Willins *et al.*, 1997;

Article published online ahead of print. Mol. Biol. Cell 10.1091/mbc.E02–06–0359. Article and publication date are at www.molbiolcell.org/cgi/doi/10.1091/mbc.E02–06–0359.

* Corresponding author. E-mail address: efimov@umdnj.edu.

[V] Online version of this article contains video material for some figures. Online version available at www.molbiolcell.org.

Abbreviations used: aa, amino acid(s); CDHC, cytoplasmic dynein heavy chain; GFP, green fluorescent protein; NUDE-C, COOH-terminal domain of the NUDE protein; NUDE-N, NH_2-terminal coiled coil domain of the NUDE protein; ts, temperature-sensitive.

Geiser *et al.*, 1997). The *Drosophila* and *Caenorhabditis elegans* homologs of NUDF have also been linked to the dynein/dynactin function (Liu *et al.*, 1999; Swan *et al.*, 1999; Lei and Warrior, 2000; Liu *et al.*, 2000; Dawe *et al.*, 2001). The mammalian homolog of NUDF, LIS1, is the product of a gene whose mutations cause lissencephaly, a brain malformation characterized by a disorganization of neurons within the cerebral cortex and a reduction in brain surface convolutions (Dobyns *et al.*, 1993; Reiner *et al.*, 1993; Chong *et al.*, 1997; Lo Nigro *et al.*, 1997; Hirotsune *et al.*, 1998). LIS1 coimmunoprecipitates with both dynein and dynactin, and colocalizes with dynein/dynactin (Faulkner *et al.*, 2000; Niethammer *et al.*, 2000; Sasaki *et al.*, 2000; Smith *et al.*, 2000; Tai *et al.*, 2002). According to two-hybrid and coexpression/coimmunoprecipitation assays, LIS1 binds two regions of the cytoplasmic dynein heavy chain (CDHC): the first AAA repeat (P1 loop) implicated in motor activity, and the N-terminal domain implicated in cargo binding (Sasaki *et al.*, 2000; Tai *et al.*, 2002). NUDF also interacts with the first AAA repeat of the *A. nidulans* CDHC in the two-hybrid system (Sasaki *et al.*, 2000) and in vitro (Hoffmann *et al.*, 2001). That NUDF might affect CDHC was first suggested by the results of a genetic screen for extragenic suppressor of a *nudF* mutation in *A. nidulans* (Willins *et al.*, 1997). Two such suppressors were mapped to the CDHC and turned out to be bypass suppressors. When observed in live *A. nidulans* cells, green fluorescent protein (GFP)-tagged CDHC and NUDF are seen at the ends of dynamic cytoplasmic microtubules as linearly moving, comet-like structures (Xiang *et al.*, 2000; Han *et al.*, 2001; Zhang *et al.*, 2002). Although the physiological significance of this localization is unclear (e.g., how it influences nuclear distribution), such localization is characteristic of dynein/dynactin and several other microtubule-interacting proteins (reviewed by Schroer, 2001; Schuyler and Pellman, 2001; Dujardin and Vallee, 2002).

The *nudF* gene was isolated inadvertently as a multicopy suppressor of the temperature-sensitive (ts) *nudC3* mutant of *A. nidulans*, in which the NUDF protein level is below normal at elevated temperatures (Osmani *et al.*, 1990; Xiang *et al.*, 1995a). The mammalian NUDC homolog binds LIS1 (Morris *et al.*, 1998) and colocalizes with cytoplasmic dynein in neurons (Aumais *et al.*, 2001). However, it is likely that the role of NUDC is not restricted to the dynein/dynactin pathway, because the *nudC* null mutant of *A. nidulans* has different and more severe growth defects than the dynein/dynactin null mutants (Chiu *et al.*, 1997).

The RO11 protein of *N. crassa* functions in the dynein/dynactin pathway (Minke *et al.*, 1999). Its *A. nidulans* homolog, NUDE, was isolated in the screen for multicopy suppressors of a *nudF* ts mutation (Efimov and Morris, 2000). At least two mammalian homologs of RO11/NUDE exist, and both are known to bind LIS1 (Feng *et al.*, 2000; Kitagawa *et al.*, 2000; Niethammer *et al.*, 2000; Sasaki *et al.*, 2000; Sweeney *et al.*, 2001). The conserved N-terminal coiled coil of NUDE is responsible for NUDF/LIS1 binding and is essential for the NUDE function, whereas its highly variable C-terminal domain is dispensable in *A. nidulans* (Efimov and Morris, 2000). Mammalian NUDE also coprecipitates and colocalizes with several dynein/dynactin subunits and centrosomal components (Feng *et al.*, 2000; Niethammer *et al.*, 2000; Sasaki *et al.*, 2000). The exact place of the NUDE protein in the dynein/dynactin pathway and how it affects NUDF/LIS1 remain to be determined.

One of the findings presented in this article is an interaction between the *nudF* and *apsA* genes of *A. nidulans*. Similar to *nud* genes, the *apsA* and *apsB* genes (*a*nucleate *p*rimary *s*terigmata) are involved in nuclear migration events in syncytial hyphae and during production of uninucleate conidia (Clutterbuck, 1994; Fischer and Timberlake, 1995; Suelmann *et al.*, 1997, 1998; Graïa *et al.*, 2000). Although both *nud* and *aps* mutants display nuclear distribution defects, a possible connection between the *aps* genes and dynein/dynactin has not been previously investigated, probably because the *aps* mutants have much milder nuclear distribution and growth defects than the *nud* mutants. However, the *S. cerevisiae* homolog of APSA, Num1p (Kormanec *et al.*, 1991), is required for dynein function in yeast (Geiser *et al.*, 1997; Heil-Chapdelaine *et al.*, 2000; Farkasovsky and Küntzel, 2001). The *apsB* gene encodes a 121-kDa coiled coil protein that does not have any obvious homologs in other organisms (Suelmann *et al.*, 1998). APSA and Num1p are large proteins consisting of coiled coil segments at the N terminus, a variable number of short repeats in the middle, and a pleckstrin homology (PH) domain at the C terminus responsible for protein targeting to the cell cortex. Both Num1p and APSA are exclusively cortical proteins, which distinguishes them from any other dynein or dynactin subunit (Farkasovsky and Küntzel, 1995; Suelmann *et al.*, 1997; Heil-Chapdelaine *et al.*, 2000; Farkasovsky and Küntzel, 2001). Localization of Num1p to the yeast cortex is independent of dynein, dynactin, and microtubules. There is growing evidence for a cortically bound form of dynein/dynactin, but only in a few cases was it possible to visualize dynein/dynactin at the cell cortex (reviewed by Dujardin and Vallee, 2002).

MATERIALS AND METHODS

Aspergillus nidulans Strains, Growth Methods, and Miscellaneous Techniques

A. nidulans strains are listed in Table 1. Genotypes of the Δ*nudE; apsA5* and Δ*nudF; apsA5* double mutants were confirmed by crosses to the wild-type R153 strain. No distinction is made in this article between the XX80 and XX80R strains (both are referred to as the *GFP::nudA* strain) or between XX87 and XX87R (both are referred to as the *GFP::nudF* strain); all four strains were used for live imaging and no differences in the GFP signal were noticed between XX80 and XX80R or between XX87 and XX87R. Standard protocols were used for handling *A. nidulans* (compiled by Kaminskyj, 2001). The complete growth media were YG (5 g/l yeast extract, 20 g/l glucose, 1 ml/l trace elements), YGK (YG plus 0.6 M KCl), YAG (YG solidified with 20 g/l agar), and YAGK (YAG plus 0.6 M KCl). The defined minimal medium was nitrate salts with 20 g/l glucose, trace elements, and necessary supplements (M-glucose). To induce expression of genes controlled by the *alcA* promoter, the following carbon sources were used in minimal media instead of glucose: 100 mM threonine (M-threonine), 1% (vol/vol) glycerol (M-glycerol) plus 50 mM methyl ethyl ketone or 2% (vol/vol) ethanol (high level of induction), 100 mM threonine plus 10 mM glucose (intermediate level of induction), and 1% (vol/vol) glycerol (low level of induction).

To accurately compare growth rates of different *A. nidulans* strains and transformants, spores were point inoculated in the center of 10-cm Petri dishes with YAG or M-glucose solid medium plus required supplements and incubated at 37°C. Colony diameters were measured on the back of plates with a ruler every 24 h for up

Table 1. *A. nidulans* strains

Strain	Genotype	Source
20.3.10	*pyrG89; argB2; pabaA1; fwA1*	G.S. May
GR5	*pyrG89; pyroA4; wA3*	G.S. May
WT	*pyrG89; yA2*	Efimov and Morris, 1998
R153	*pyroA4; wA3*	C.F. Roberts
AO1	*nudC3; pyrG89; pabaA1; nicA2; wA2*	Osmani *et al.*, 1990
C3y-3	*nudC3; pyrG89; yA2*	AO1 × WT
XX3	*nudA1; pyrG89; chaA1*	Xiang *et al.*, 1994
XX5	*nudA2; pyrG89; chaA1; wA3*	Xiang *et al.*, 1995a
XX8	*nudA4; pyrG89; chaA1; wA3*	Xiang *et al.*, 1994
A5.4	*nudA5; pyrG89; yA2*	Efimov and Morris, 1998
WX317	*nudK317; pyrG89; yA2*	Xiang *et al.*, 1999
WX416	*nudI416; pyrG89*	Xiang *et al.*, 1999
XX20	*nudF6; pyrG89*	Xiang *et al.*, 1995a
XX21	*nudF7; pyrG89; yA2*	Xiang *et al.*, 1995a
ΔF54	Δ*nudF*::*pyr4; pyrG89; pyroA4; wA3*	Willins *et al.*, 1995
SF2-9	Δ*nudE*::*argB; pyrG89; argB2; pabaA1; fwA1*	Efimov and Morris, 2000
SF2-9-9	Δ*nudE*::*argB; pyrG89*	SF2-9 × GR5
AJC1.8	*apsB14; biA1*	Clutterbuck, 1969
apsB14-2	*apsB14; pyrG89*	AJC1.8 × GR5
AJC1.3	*apsA5; biA1*	Clutterbuck, 1969
apsA5	*apsA5; pyrG89; yA2*	AJC1.3 × A5.4
SRF23	*apsA1; pyrG89; pabaA1; yA2; wA3*	R. Fischer
SRF30	Δ*apsA*::*pyr4;* Δ*argB*::*trpC*Δ*B; pabaA1; pyroA4; yA2; wA3*	Suelmann *et al.*, 1997
apsA5/E-1, 2, 4	Δ*nudE*::*argB; apsA5; pyrG89; (yA2)*	apsA5 × SF2-9-9
apsA5/ΔF-1, 2, 12, 19	Δ*nudF*::*pyr4; apsA5; pyrG89; (yA2); (wA3)*	apsA5 × ΔF54
XX80	*alcA(p)*::*GFP*::*nudA*::*pyr4; pyrG89; pyroA4; wA3*	Xiang *et al.*, 2000
XX87	*alcA(p)*::*GFP*::*nudF*::*pyr4; pyrG89; pyroA4; wA3*	Han *et al.*, 2001
XX80R	*alcA(p)*::*GFP*::*nudA*::*pyr4; pyrG89; argB2*	XX80 × 20.3.10
XX87R	*alcA(p)*::*GFP*::*nudF*::*pyr4; pyrG89; argB2*	XX87 × 20.3.10
XX80RE	*alcA(p)*::*GFP*::*nudA*::*pyr4;* Δ*nudE*::*argB; pyrG89; argB2; (fwA1)*	XX80R × SF2-9
XX87RE	*alcA(p)*::*GFP*::*nudF*::*pyr4;* Δ*nudE*::*argB; pyrG89; argB2*	XX87R × SF2-9
ΔF/GFP-*nudA*	Δ*nudF*::*pyr4; GFP*::*nudA*::*pyr4; pyrG89; pyroA4; wA3*	Zhang *et al.*, 2002
XX21pSAL#2	XX21 + 2 copies of pSAL-1 at the *nudE* locus	XX21 transformation
XX21pSAL#13	XX21 + 4÷5 copies of pSAL-1 at the *nudE* locus	XX21 transformation

to 5 d. The increase in colony diameter from day 1 to day 5 was linear (coefficients of determination were typically >0.9995) and was used to calculate the colony radial growth rate. The SE of these measurements was <0.4 mm/d in each individual experiment, as estimated from the error of slope calculations and from the variation among duplicate plates or among independent transformants. Alternatively, colony diameters were calculated from the colony areas, which were measured after taking images of colonies. The latter method was used to compare growth rates of the SF2-9-9 (Δ*nudE*) strain transformed with pAid, pAid::*nudE*, and pAid::*nudF*.

Determination of the effect of multiple copies of different genes on different *A. nidulans* mutants was done routinely as follows. The mutants, each unable to grow without uridine and uracil due to the *pyrG89* mutation, were transformed with the pAid-derived plasmids. At least four independent transformants were gridded together with control transformants on YAG and YAGK plates and incubated at 32, 37, and 43°C for 3 d. All ts mutants used in this work are somewhat suppressed by 0.6 M KCl, so that YAGK is a less restrictive condition than YAG at the same temperature. The colony sizes and conidiation of the transformants were compared with those of the controls. The main control was the same strain transformed with the empty vector pAid. As a wild-type control, transformants GR5[pAid], SF2-9-9[pAid::*nudE*], XX21[pAid::*nudF*], apsA5[pAid::*apsA*], and C3y-3[pAid::*nudC*], all of which grow at the same rate, were used. The SRF30 (Δ*apsA*) strain was transformed with the pAid2-14 clones (selection for arginine prototrophy) and transformants were analyzed on M-glucose plus pyridoxine and *p*-aminobenzoic acid. The colony radial growth rates of some transformants were also compared quantitatively as described above.

Transformation of *A. nidulans* was done using germinating conidia essentially as described previously (Osmani *et al.*, 1987). *A. nidulans* genomic DNA was prepared according to Willins *et al.* (1995) with minor modifications. For 4,6-diamidino-2-phenylindole (DAPI) staining of nuclei in conidia, a suspension of conidia was spread on a cover glass, allowed to dry (~20 min at 55°C), and stained with DAPI according to a standard protocol (Willins *et al.*, 1995).

Plasmids

A. nidulans autonomously replicating multicopy plasmids used in this work are based on either pAid or pAid2-14 vector and are written as pAid::*nudF*, pAid2::*nudF*, pAid::*nudE*, and so on to indicate the gene they carry (each name refers to a unique construct). The inserts are *A. nidulans* genomic DNA fragments at the *Bam*HI site of either pAid or pAid2-14. pAid (Xiang *et al.*, 1999; Efimov and Morris, 2000) is an AMA1-bearing, autonomously replicating plasmid pHELP1 (Gems *et al.*, 1991; Gems and Clutterbuck, 1993) plus the *pyrG* gene as a selective marker. pAid2-14 is pHELP1 plus the *argB* gene as a selective marker. In pAid2-14, the 1.7-kb *Bam*HI-*Xho*I fragment from pMS12 (Fungal Genetics Stock Center, Kansas City, KS) is inserted at the *Bgl*II site of pHELP1 (all ends were filled in before ligation) with the *argB* gene oriented away from the AMA1.

pAid::*nudF6* and pAid::*nudF* were isolated in screens for multicopy suppressors of the *nudF7* mutation (Efimov and Morris, 2000) and the Δ*nudE* mutation (this work), respectively. The insert in pAid::*nudF* contains the *nudF* gene (1.3 kb, oriented toward AMA1), ~3 kb of upstream sequence, and ~5.5 kb of downstream sequence. To make pAid2::*nudF*, the ~7 kb *Aat*II-*Bgl*II fragment from pAid::*nudF* was inserted at the *Aat*II-*Bam*HI sites of pAid2-14, resulting in an insert that is the same as in pAid::*nudF*, but carries ~2.6 kb less of the sequence downstream of *nudF*. The ~5-kb insert in pAid::*nudF6* contains the *nudF6* ts allele of the *nudF* gene and flanking regions.

pAid::*nudC* and pAid::*nudC*Δ were isolated in the screen for multicopy suppressors of the *nudC3* mutation (this work). The insert in pAid::*nudC* is ~8 kb and contains the *nudC* gene and flanking regions. The insert in pAid::*nudC*Δ is ~6 kb, contains most of the *nudC* gene (oriented away from AMA1), and terminates inside the last intron of the *nudC* gene (the sequence of the *nudC*/vector junction is gcattgtgct/gatccccgggtacc. . .).

The insert in Aid::*apsA* and pAid2::*apsA* is the 10.5-kb *Bam*HI-*Bam*HI fragment from pRF7 (Fischer and Timberlake, 1995) with the *apsA* gene and flanking regions.

pAid::*nudE* (Efimov and Morris, 2000), pAid::*GFP*::*nudE*, pAid::*GFP*::*nudE-N*, pAid::*GFP*::*nudE-C* were made by subcloning and are identical to each other except for the *GFP* gene or deletions within the *nudE* gene. To create *GFP*::*nudE* fusions, codons 3–238 of the adapted for plants GFP version GFP2-5 (Fernández-Ábalos *et al.*, 1998) were amplified by polymerase chain reaction (PCR) from the plasmid pMCB4 (provided by John H. Doonan, John Innes Centre, Norwich, United Kingdom) and inserted after the third codon of the *nudE* gene by using PCR-mediated recombination. In-frame deletion of aa 45–214 in the NUDE-C variant was obtained by deleting the *Nru*I-*Bgl*II fragment (579 base pairs after filling in). The C-terminal domain of NUDE (aa 216–586) was deleted in the NUDE-N variant by excising the *Bgl*II-*Mfe*I fragment (539 base pairs after filling in). The latter deletion disrupts the *nudE* ORF, resulting in termination of the NUDE sequence after aa 215 and addition of 16 new aa. The cloning junctions and the regions amplified by PCR were verified by sequencing.

pAid clones with the *GFP**::*nudE* fusions are identical to the plasmids with the *GFP*::*nudE* fusions described above except for a point mutation in the *GFP* gene introduced during PCR. The mutation in the *GFP** gene changes Leu-42 of the GFP2-5 protein to His. The plasmid pSAL-1 was used to integrate the *GFP**::*nudE* gene into the *A. nidulans* genome under the *alcA* promoter. It is pAL3 vector (Waring *et al.*, 1989) carrying a 3.7-kb insert at the *Bam*HI site with the *GFP**::*nudE* fusion (oriented away from *alcA*), 0.27 kb of the sequence upstream of the *nudE* gene, and 0.9 kb of the sequence downstream of *nudE*.

Screens for Multicopy Suppressors of ΔnudE and nudC3 Mutations

The SF2-9-9 (Δ*nudE*) strain was transformed with its own genomic DNA fragments (5–20-kb sucrose gradient fraction of *Sau*3AI partial digest) ligated to the pAid vector (cut with *Bam*HI and dephosphorylated). Transformants were plated in YAGK at 43°C and overlaid with YAG the next day. The total number of transformants was $>2\times10^4$. Six clones with suppressed phenotypes were identified by their improved conidiation, resulting in a patch of green color in the poorly conidiating mycelium. Three clones had completely suppressed, wild-type phenotypes. The suppressor plasmids were recovered from two of them and were found to contain overlapping inserts with the *nudF* gene and no *nudE* or *nudC* genes. Three other suppressed clones were similar to each other and had slightly improved conidiation. Suppressor plasmids recovered from them contained overlapping inserts with a novel gene and no *nudE*, *nudF*, or *nudC* genes.

The ts C3y-3 (*nudC3*) strain was transformed with genomic DNA fragments from the XX20 (*nudF6*) mutant (5–20-kb sucrose gradient fraction of *Sau*3AI partial digest) ligated to the pAid vector (cut with *Bam*HI and dephosphorylated). Several growth conditions were tried to find the least restrictive condition with low conidiation level. The bulk of transformants was plated in YAGK at 37°C, overlaid with YAGK the next day, and shifted to 43°C after two more days at 37°C. Alternatively, the plates were overlaid with either YAG or YAGK and left at 37°C. The total number of transformants was $>1.5\times10^5$. Suppressed transformants were identified as patches of yellow color brighter than the background. Approximately 160 clones were completely suppressed and were deemed to had been transformed with the *nudC* gene. The suppressing plasmids were recovered from five such clones and each was found to carry the full-length *nudC* gene. Plasmids from four strongly (but not completely) suppressed transformants were found to carry inserts with the 3′-truncated *nudC* gene, as evidenced by restriction mapping and PCR with the *nudC*-specific primers. The truncation site was determined in one such plasmid, pAid::*nudC*Δ, by sequencing the insert ends. Plasmids from three weakly suppressed clones were found to carry overlapping inserts with the same novel gene that was isolated in the screen for multicopy suppressors of the Δ*nudE* mutation. The suppressing plasmids could not be recovered from several transformants, including six clones phenotypically different from the clones described above.

Protein Extraction and Immunoblotting

To extract *A. nidulans* total protein, mycelium was collected from liquid cultures by filtration after ~20 h of growth, washed with distilled water, pressed dry, and ground to a powder with mortar and pestle in liquid nitrogen. The ground mycelium was resuspended and boiled in the urea/SDS buffer (Osherov and May, 1998): 1% SDS, 9 M urea, 25 mM Tris-HCl (pH 6.8), 1 mM EDTA, and 0.7 M 2-mercaptoethanol. Alternatively, mycelium was resuspended in the urea/SDS buffer with 1% (vol/vol) protease inhibitor cocktail for fungal and yeast cells (Sigma-Aldrich, St. Louis, MO) and then ground and boiled. The debris was removed by centrifugation in a microcentrifuge. Protein concentrations were estimated with the bicinchoninic acid protein assay kit (Pierce Chemical, Rockford, IL) by using bovine serum albumin as a standard. To block thiol groups, which interfere with the assay, extracts were diluted at least 50-fold in 0.5 M iodoacetamide, 0.1 M Tris-HCl, pH 9.5.

GFP fusions were detected on Western blots using purified rabbit anti-GFP polyclonal antibody (Torrey Pines Biolabs, Houston, TX). An affinity-purified rabbit polyclonal antibody against the NUDF protein (Xiang *et al.*, 1995a) was a gift from Xin Xiang (Uniformed Services University of the Health Sciences, Bethesda, MD). An alkaline phosphatase conjugate was used as a secondary antibody. Detection was performed with BCIP/NBT (5-bromo-4-chloro-3-indolyl-phosphate/nitroblue tetrazolium) phosphatase substrate system (KPL, Gaithersburg, MD).

Fluorescence Microscopy and Live Imaging of A. nidulans

Different methods of growing *A. nidulans* for live imaging were used with comparable results. Originally, Petri dishes with a hole in the bottom covered with a coverglass and sealed with a mixture of paraffin, lanolin, and Vaseline (1:1:1) were used to grow and observe hyphae in liquid media. Later, Delta TPG culture dishes (Bioptechs, Butler, PA) were found to be more convenient. Agar pads were used to observe hyphae on solid media. Glass slides were placed into Petri dishes and overlaid with a solid growth medium to produce a layer 1–1.5 mm in thickness. Pieces of wet paper were put in the dishes to slow down drying of agar during incubation. Conidia were diluted with the growth medium, and 10 μl (10^4–10^5 conidia) were placed on the agar pads. After incubation, a drop of liquid medium was placed on the hyphae and they were covered with a 22-mm-round coverglass. The agar around the coverglass was removed, and the slide was placed on the microscope with the cov-

erglass toward the objective. This agar pad method was later modified as follows. Agarose was used instead of agar; liquid medium was sterilized by filtration, and agarose was added to 1% (wt/vol) and dissolved by boiling. Pads were prepared as described above. For observation, a piece of the agarose layer with hyphae was cut out and gently placed, cell side down, into Bioptechs' Delta TPG culture dish or on a 50 × 45-mm coverglass on a drop of liquid medium. Some dislodging of the mycelium was inevitable during this process.

The microscope setup for observing GFP-tagged proteins in live *A. nidulans* hyphae was identical to that used by Xiang and colleagues (Xiang *et al.*, 2000; Han *et al.*, 2001; Zhang *et al.*, 2002), except that the sample temperature was controlled by an air-heated chamber enclosing the microscope rather than by a heated stage. It was an Olympus IX70 inverted fluorescence microscope equipped with 5 MHz MicroMax cooled charge-coupled device camera (Princeton Instruments, Trenton, NJ), a shutter, and a controller unit connected to a Macintosh computer. A fluorescence filter cube for fluorescein isothiocyanate and 100× objectives were used. Unless stated otherwise, cells were grown and observed at 32°C on agarose pads after 23–26 h of incubation. At least four samples of each strain were examined. For each sample, time-lapse series were recorded for 8–15 individual hyphae first and then several hundreds of hyphae were examined by eye for the presence of fluorescent structures and more series were recorded if necessary. IPLab software (Scanalytics, Fairfax, VA) was used to acquire images and time-lapse series of GFP fluorescence. Images and series were acquired using identical microscope and camera settings. Images represented the first exposure of cells to the excitation light (the signal fades after prolonged exposure). Each time-lapse series was recorded shortly after taking the first image shown in the figure. For reproduction, images and series were converted to 8-bit format, and unless stated otherwise, used without modifying the intensities. Unless stated otherwise, the exposure time for images and series was 0.1 s, the time between exposures in series was 2 s, and the number of exposures was 30. The series were sped up fivefold during conversion into QuickTime videos. In Videos 5, A and B, 100 pixels equals 6.79 μm. In all other Videos, 100 pixels equals 6.69 μm.

RESULTS

A Modified Procedure for Live Imaging of the GFP::nudF and GFP::nudA Strains of A. nidulans

The *GFP::nudF* and *GFP::nudA* strains have been constructed and studied by Xiang and colleagues (Xiang *et al.*, 2000; Han *et al.*, 2001; Zhang *et al.*, 2002). Both the GFP::NUDF and GFP::NUDA fusions localize to unidirectionally moving dashes or streaks that coincided with microtubule ends. These moving structures will be referred to as "comets." Herein, the *GFP::nudF* and *GFP::nudA* strains of *A. nidulans* are compared with the *GFP::nudF;* Δ*nudE* and *GFP::nudA;* Δ*nudE* strains. The latter two strains were obtained by crossing the first two strains to a strain with a deletion of the *nudE* gene (Efimov and Morris, 2000).

In this work, the conditions for live imaging of the *GFP::nudF* and *GFP::nudA* strains have been modified as follows. First, cells were grown on the surface of solid media rather than in liquid media. This allowed observations of isolated hyphal tips at the colony margin, as well as of the internal hyphal segments closer to the center of the colony. Unless stated otherwise, the hyphal tips selected for figures and videos were from the periphery of the colony. Second, threonine was used as a carbon source instead of glycerol to overexpress the GFP fusions. The transcription of the *GFP::nudF* and *GFP::nudA* genes is controlled by the inducible *alcA* promoter, whose activity is repressed by glucose and induced by alcohols (Creaser *et al.*, 1985; Waring *et al.*, 1989). Glycerol neither represses nor induces the *alcA* promoter. In contrast, threonine is a potent inducer of the *alcA* promoter (Creaser *et al.*, 1985). Thus, the induction levels of the *GFP::nudF* and *GFP::nudA* genes used in this work should be much higher than in the previous studies (Xiang *et al.*, 2000; Han *et al.*, 2001; Zhang *et al.*, 2002). It was estimated from immunoblots that the level of the GFP::NUDF protein was similar to the wild-type NUDF level in cells grown on glycerol, but was 20–40 times higher in cells grown on threonine (our unpublished data). The intensity of GFP fluorescence varied between different experiments and between different hyphae within the same sample when glycerol was used. Such variability was not observed when threonine was used.

Deletion of nudE Gene Does Not Eliminate Comet-Like Structures of GFP::NUDF Fusion

The behavior of the GFP::NUDF fusion was identical in the *GFP::nudF* and GFP*::nudF;* Δ*nudE* strains when they were grown on a strongly inducing threonine medium (Figure 1, A and B, and Video 1, A and B). The GFP signal was distributed throughout the cytoplasm. The darker regions could be vacuoles, mitochondria, and nuclei. Despite the bright background, the comet-like structures (Han *et al.*, 2001) were seen in time-lapse series, particularly near the tips (Videos 1, A and B).

The experiments described further in this work reveal that the *nudE* deletion is completely suppressed by the overexpression of the NUDF protein. Consistent with this finding, the *GFP::nudF;* Δ*nudE* strain was identical to the *GFP::nudF* strain when grown on threonine (high *GFP*::*nudF* induction), but was inhibited compared with the *GFP::nudF* strain when grown on glycerol (low *GFP*::*nudF* induction). In contrast, the *GFP::nudA;* Δ*nudE* strain was inhibited compared with the *GFP::nudA* on both threonine and glycerol. It was not possible to compare GFP::NUDF behavior in the *GFP::nudF* and *GFP::nudF;* Δ*nudE* strains grown on glycerol, due to the mentioned high variability of the GFP signal among different hyphae. In addition, the background fluorescence was often higher in the *GFP::nudF;* Δ*nudE* strain when grown on glycerol, possibly due to a positive selection for a higher level of *GFP*::*nudF* induction. To bring down the GFP::NUDF fusion level, threonine (100 mM) was used in combination with the *alcA* repressor glucose (10 mM). On the threonine plus glucose medium, the *GFP::nudF;* Δ*nudE* strain was inhibited compared with the *GFP::nudF* strain, whereas the *GFP::nudF* strain seemed normal. Again, the comets were present in the *GFP::nudF;* Δ*nudE* strain (Figure 1D and Video 1D), and no differences were obvious between the GFP*::nudF;* Δ*nudE* and *GFP::nudF* strains. The background fluorescence was lower, giving comets more contrast. Also, cells grew more vigorously in the presence of glucose (notice that the tip visibly elongates in Video 1D). Unfortunately, some variability in the background fluorescence among different hyphae was present when threonine was used in combination with glucose, thus making thorough comparisons of the two strains problematic.

Previous studies of the GFP-tagged NUDF and dynein/dynactin subunits described the comets near hyphal tips (Xiang *et al.*, 2000; Han *et al.*, 2001; Zhang *et al.*, 2002). Figure

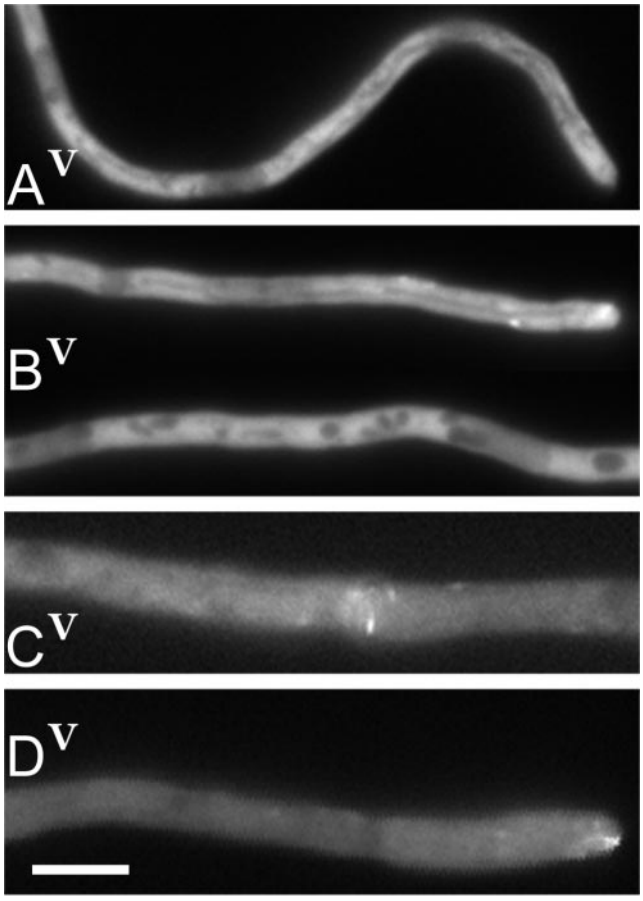

Figure 1. Deletion of the *nudE* gene does not abolish the GFP::NUDF fusion localization to comet-like structures in *A. nidulans* hyphae. (A) The control *GFP::nudF* strain grown on the strongly inducing threonine medium. Despite the bright background, the comets can be seen in the video near the tip. (B) Hyphae of the *GFP::nudF;* Δ*nudE* strain were grown as described in A. Video shows the tip of the top hypha with several comets clearly visible. (C) The control *GFP::nudF* strain grown on threonine plus glucose to bring down the expression of the fusion. This is a region ~200 μm away from the hyphal tip. The comets are clearly seen in the video. The significance of a structure in the center is not clear. (D) Typical example of a hyphal tip of the *GFP::nudF;* Δ*nudE* strain grown as described in C. The tips of the *GFP::nudF* strain looked the same. Bar, 5 μm.

1C and Video 1C show a hyphal segment ~200 μm away from the tip. Clearly, the GFP::NUDF comets are present there and move in all directions. However, the comets were typically the brightest and most easy to observe near the tips (e.g., Figure 1D and Video 1D).

Deletion of nudE Gene Does Not Eliminate Comets of GFP::NUDA, but Affects Their Behavior

The *GFP::nudA* hyphae did not have such an intense background fluorescence as the *GFP::nudF* hyphae when grown on threonine. The comets of the GFP::NUDA fusion (Xiang *et al.*, 2000) were present in almost every hyphal tip (Figure 2A1–3 and Video 2A1) and were also seen on many occasions in the internal hyphal segments. In still images, the tip comets showed as one or two bright dots at the very tip. The comets were also present in the *GFP::nudA;* Δ*nudE* strain, but their behavior was changed. The tips of the *GFP::nudA;* Δ*nudE* strain usually contained a large patch of fluorescence with several long streaks (Figure 2B1–4). The patch was sometimes at a distance from the tip (Figure 2B2). Time-lapse series showed that the comets were longer, more abundant, and oriented more randomly than in the control strain (Video 2B1 and 2B2; not included videos for Figure 2B3 and 2B4 show a similar behavior). Often, a diffuse background fluorescence was present around the cluster of comets (Figure 2B1 and 2B2 and Video 2B1 and 2B2). These changes in the behavior of GFP::NUDA in the presence of the Δ*nudE* mutation were also obvious when the strains were compared on a less inducing glycerol medium (our unpublished data). The clusters of comets situated proximal to the tip (such as in Video 2B2) and in the internal hyphal segments were also common in the *GFP::nudA;* Δ*nudF* strain (our unpublished data), and were never seen in the control *GFP::nudA* strain.

Overexpression of GFP::NUDA Fusion Results in Appearance of "Specks"

In addition to comets, new structures were observed in the *GFP::nudA* hyphae grown on threonine. They were little dots present in the internal hyphal segments (Figure 2C). Unlike the comets, which always moved unidirectionally, the dots were either immobile or bounced randomly. Such structures will hereafter be referred to as specks. Video 2C shows a comet moving at a constant speed from left to right (the left side of the field), and apparently colliding with a pair of specks that are jiggling around. The specks were never observed when the *GFP::nudA* strain was grown on glycerol, even when the comets were present, suggesting that the specks require a high fusion expression to develop or to become visible. The specks were also observed in the *GFP::nudA;* Δ*nudE* hyphae grown on threonine.

NUDE Protein Is Targeted to Comets by Its C-Terminal Domain

The NUDE protein is composed of two distinct domains (Efimov and Morris, 2000). The N-terminal domain (NUDE-N, ~200 aa) is predicted to form a coiled coil, is evolutionarily conserved, and binds NUDF/LIS1. In *A. nidulans*, it is almost as functional as the full-length protein when expressed from a multicopy plasmid. The NUDE C-terminal domain (NUDE-C) that follows the coiled coil varies in length and sequence among different species and is basic and serine rich. The C-terminal domain is not functional by itself.

To examine intracellular localization of the full-length NUDE protein and its N- and C-terminal domains, these were fused to the GFP and placed on the multicopy plasmid under the native *nudE* promoter (Figure 3A). The plasmids expressing the GFP::NUDE and GFP::NUDE-N fusions suppressed the Δ*nudE* and *nudF7* mutations, whereas the GFP::NUDE-C fusion did not (Figure 3A). All three constructs were present at similar levels in total protein extracts (Figure 3B). When *A. nidulans* strains transformed with the

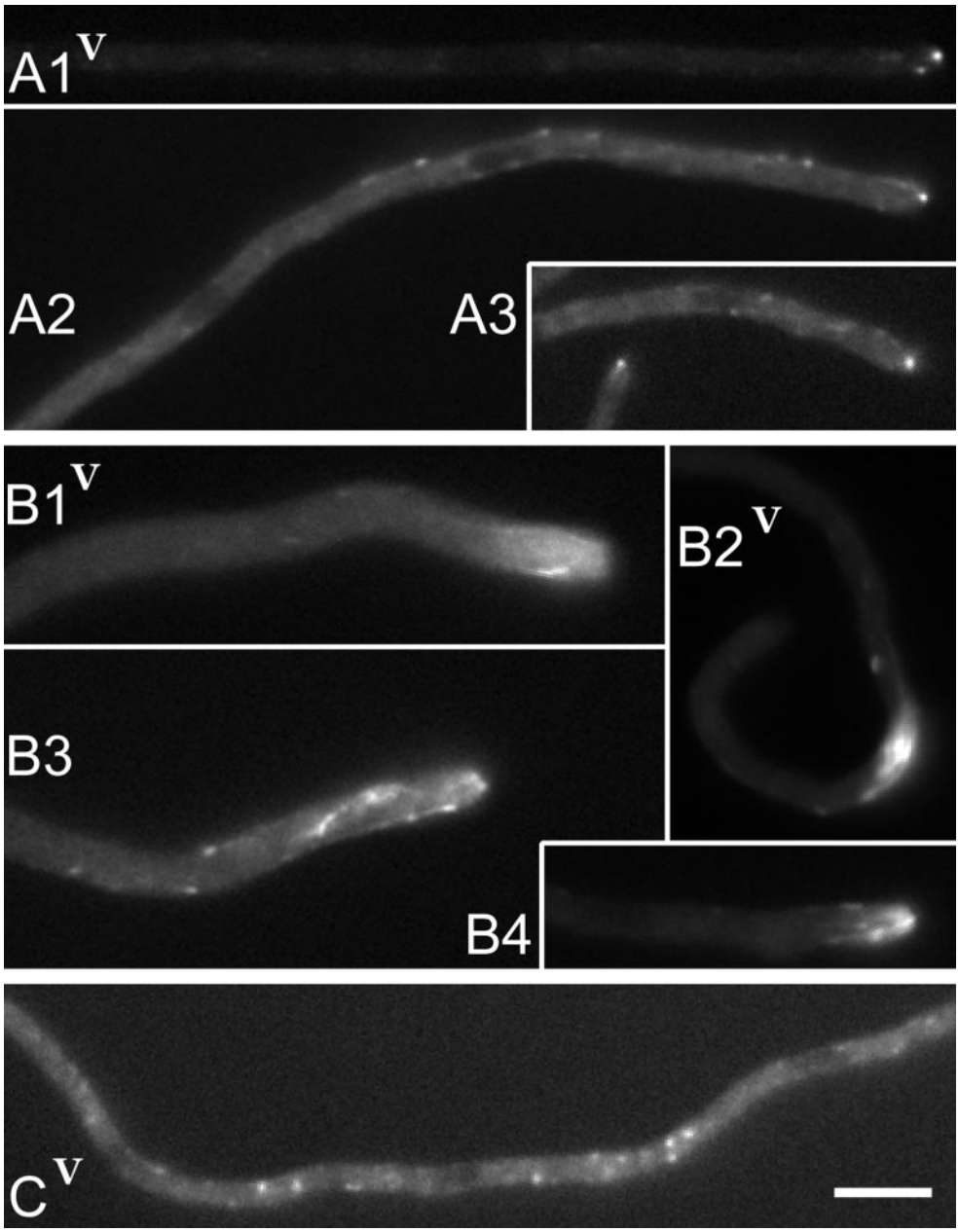

Figure 2. Deletion of the *nudE* gene does not eliminate the comets of GFP::NUDA, but changes their behavior. Hyphae were grown under identical conditions on the strongly inducing threonine medium as for Figure 1, A and B. (A) Hyphal tips of the control *GFP::nudA* strain. The intensities in Video A1 were adjusted to brighten the image. Exposure for A2 was 0.6 s. (B) Hyphal tips of the *GFP::nudA;* Δ*nudE* strain. (C) An example of specks of GFP::NUDA in the internal hyphal region of the *GFP::nudA* strain. Video shows that the specks are immobile or bounce randomly, whereas a comet moves from left to right. The exposure time for this image and video was 0.6 s. Bar, 5 μm.

above-mentioned plasmids, were examined for the GFP fluorescence, considerable variability in the fluorescence intensity was observed among different hyphae (Figure 4B shows a typical example). The most likely cause of this variability was a variation in the copy number of the *A. nidulans* autonomously replicating plasmid due to its mitotic instability (Gems *et al.*, 1991). The fluorescence intensity was always the same along the length of each individual hypha, apparently because the septa that divide the hyphae into compartments are perforated and allow passage of cytoplasm. Due to the extreme variability of the levels of the GFP-tagged proteins among different hyphae, the conclusions about the localization of the GFP::NUDE constructs had to be qualitative. That is, it was possible to determine whether particular structures (e.g., comets) were present, but the abundance and intensity of structures were different in each hypha. One benefit of this variability was that a broad range of expression levels could be examined within the same sample.

The full-length GFP::NUDE localized to comet-like structures identical to those of the GFP::NUDA and GFP::NUDF (Figure 4A). Close to hyphal tips, the comets tended to move predominantly toward the tip and were typically the brightest at the tip. The comets were readily observed proximal to the tips and in the internal compartments, where they moved in both directions. Video 4A shows several comets moving in opposite directions. The specks were also ob-

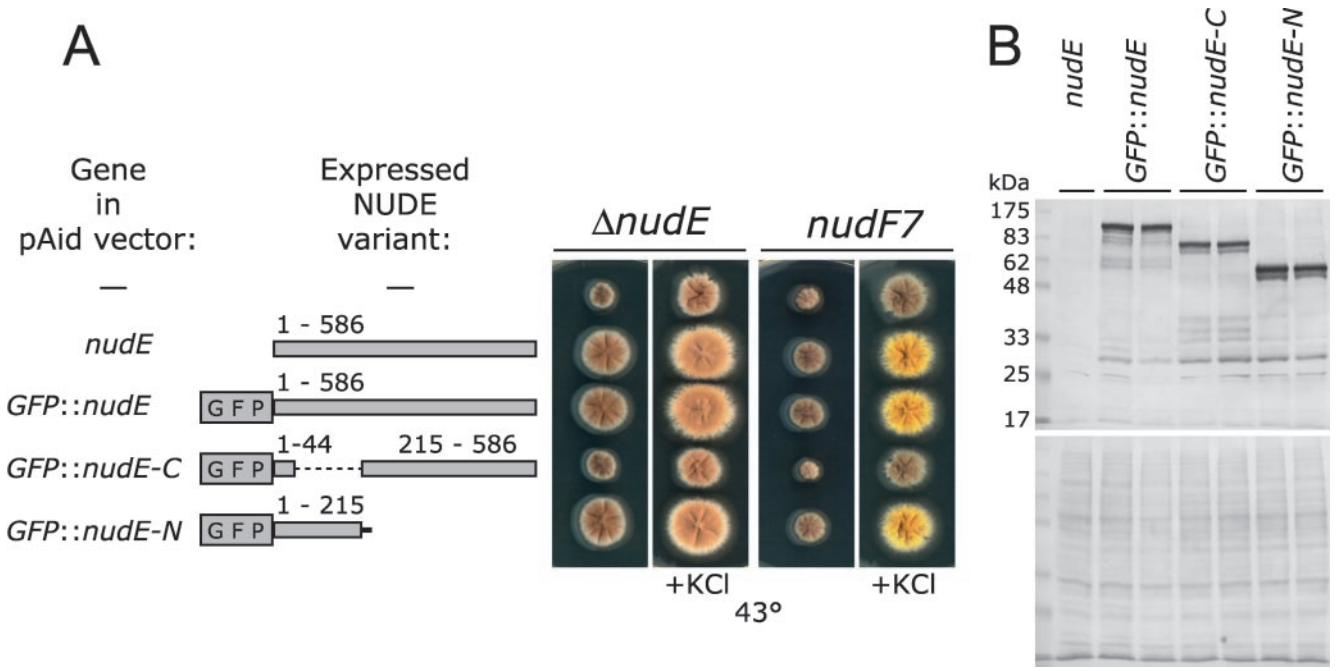

Figure 3. (A) Biological activities of the GFP-tagged NUDE protein variants. A *nudE* deletion strain (SF2-9) and the *nudF7* ts mutant (XX21) were transformed with indicated genes in the multicopy vector pAid. Transformants were grown for 3 d on complete medium (YAG) without or with 0.6 M KCl at 43°C, which is a restrictive temperature for the *nudF7* mutant. The fawn color of conidia in the Δ*nudE* strain is similar to the brownish color of nonconidiating mycelium. The color of conidia in the *nudF7* strain is yellow. (B) GFP::NUDE variants are expressed at similar levels. Total protein extracts were made from a Δ*nudE* strain transformed with indicated genes in the pAid vector. Two different transformants were used for each GFP::NUDE variant. Proteins (12 μg/lane) were separated on a 10% SDS-PAGE and immunoblotted with an anti-GFP antibody. The bottom panel is Ponceau S staining of the membrane after protein transfer.

served in older hyphal regions, where they coexisted with comets. The specks of GFP::NUDE behaved like the specks of the GFP::NUDA (Video 2C) and are described in detail below.

The nonfunctional GFP::NUDE-C also localized to comets (Figure 4C and Video 4C). These comets resembled those of the GFP::NUDA in the Δ*nudE* background in that they were more disorganized compared with the GFP::NUDE comets. This was expected because the expression was done in a Δ*nudE* mutant, and GFP::NUDE-C does not complement it. The specks were never observed with the GFP::NUDE-C fusion. Instead, judging from the fact that the maximum background fluorescence inside hyphae with GFP::NUDE-C was higher than with GFP::NUDE, the excess of the GFP::NUDE-C fusion distributed uniformly.

The functional GFP::NUDE-N fusion was observed only as a uniform fluorescence throughout the cytoplasm (Figure 4B). Hyphae with different levels of fluorescence were examined, and neither comets nor specks could be detected either in still images or in time-lapse series. Occasionally, the GFP signal seemed to accumulate in nuclei, but that did not happen in every hypha.

Specks of Full-Length GFP::NUDE Fusion

An accidentally created mutant version of GFP made it possible to observe NUDE specks independently from comets. The GFP mutant designated GFP* has histidine instead of leucine at position 42 because of a point mutation introduced during PCR. The GFP*::NUDE, GFP*::NUDE-C, and GFP*::NUDE-N fusions were made as the GFP fusions described above and behaved just like them in complementation assays shown in Figure 3A. However, none of the three GFP* fusions could be observed in comets. On the other hand, the specks were readily observed with the GFP*::NUDE. The fusions GFP*::NUDE-C and GFP*::NUDE-N showed only uniform localization similar to that of GFP::NUDE-N. How the mutation affected the physical properties of GFP is not known. Were it to reduce the brightness of GFP, it could have made the comets invisible, while still allowing observation of specks. This is because, compared with comets, the specks of GFP::NUDE were often much brighter and more resistant to fading upon prolonged exposure to the excitation light. When the GFP*::NUDE fusion was expressed from a multicopy plasmid, individual hyphae varied greatly in the abundance and intensity of specks. To stabilize GFP*::NUDE expression, the *GFP*::nudE* gene was placed under the control of the *alcA* promoter and integrated into the chromosome at the *nudE* locus. The resulting strains contained specks in every hypha even when grown on a noninducing glycerol.

Figure 5A and Video 5A show a typical example of specks and their movements. The brightness of specks varied significantly, but even the brightest specks were sharp and tiny. Very bright specks may show as large round objects due to

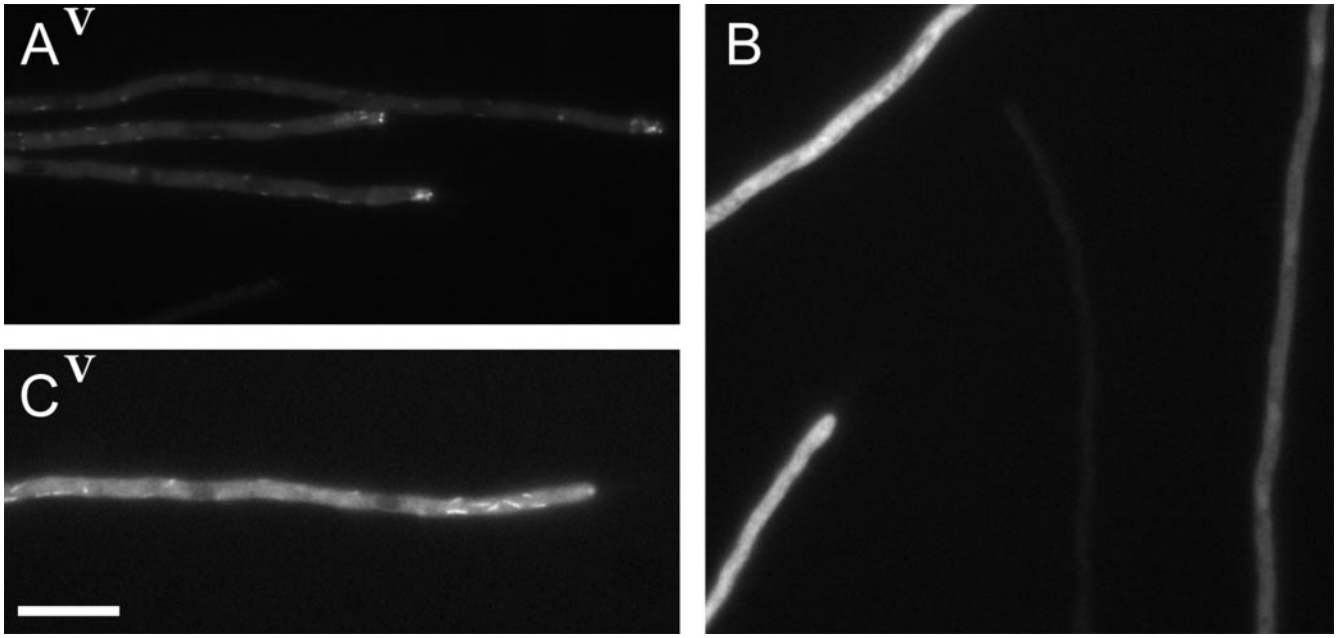

Figure 4. GFP-tagged NUDE and NUDE-C localize to comets, whereas NUDE-N distributes uniformly throughout the cytoplasm. A Δ*nudE* strain was transformed with pAid::*GFP*::*nudE*, pAid::*GFP*::*nudE-N*, and pAid::*GFP*::*nudE-C* (Figure 3A) and transformants were grown on a threonine medium as described for Figures 1, A and B, and 2. (A) Full-length GFP::NUDE fusion. The brightness of the image was slightly increased to show faint comets far from the tip. The video shows comets moving in both directions parallel to the hypha axis. The background fluorescence inside this hypha is typical for this fusion and never was as bright as in C or B. (B) GFP::NUDE-N. This is an example of GFP signal variability among individual hyphae. All four hyphae are in the same focal plane. (C) GFP::NUDE-C. The video shows that many comets move at an angle to the hypha axis. Bar, 10 μm.

image reproduction artifacts. The movements of specks were jerky and unpredictable. The net result of the movements was that the specks distributed uniformly along the hypha. Interestingly, specks often moved in pairs as if they were connected. A thin line of fluorescence was sometimes seen between adjacent specks. Destabilization of microtubules with benomyl (4 μg/ml, 2–5 h at 28°C) did not eliminate the specks, but completely stopped their movement (Figure 5B and Video 5B). In older hyphae, the specks were incorporated into bright cables (Figure 5C). No movements were seen in such cables.

Multiple Copies of nudF Gene Completely Suppress Deletion of nudE Gene

Deletion of the *nudE* gene results in morphological defects characteristic of *A. nidulans* dynein deletion mutants (impaired nuclear migration and distribution, decreased colony radial growth rate, reduced conidiation), but each defect is less severe than in the Δ*nudA* or Δ*nudF* strains (Efimov and Morris, 2000). Unlike the latter strains, which produce very few conidia (roughly 0.01% of wild-type amounts), the Δ*nudE* strains produce sufficient amounts of conidia (up to 1% of wild-type amounts on YAGK plates) to make their transformations possible. Conidia obtained from the Δ*nudE* strains were bigger than those from the wild-type control and often contained two or more nuclei, in contrast to the always uninucleate wild-type conidia (our unpublished data). Such changes in conidial morphology were also observed in the *nudF* and *nudA* ts mutants grown under partially restrictive conidiation, in *apsA* mutants (our unpublished data), and have been described in a dynactin mutant of *Aspergillus oryzae* (Maruyama *et al.*, 2002). Due to the availability of conidia, an efficient transformation of the Δ*nudE* mutant could be achieved and that made possible a screen for multicopy suppressors of the Δ*nudE* mutation by using a strategy that previously led to the isolation of the *nudE* gene (Efimov and Morris, 2000). The strategy relies on the *A. nidulans* transformation with random genomic DNA fragments ligated in vitro to the *A. nidulans* autonomously replicating multicopy vector (Gems *et al.*, 1991). This cloning method, originally developed to facilitate gene cloning by complementation (Efimov and Morris, 1998), bypasses genomic library construction in another host, results in efficient transformations and insert sizes up to 15–20 kb, and minimizes the chances of plasmid rearrangement during transformation (Gems and Clutterbuck, 1993), thereby permitting recovery of plasmids from the transformants.

A Δ*nudE* strain producing green conidia was transformed with its own genomic DNA fragments in the multicopy vector pAid. Suppressed colonies were identified on transformation plates as patches of green color resulting from enhanced conidiation in the background of brownish, poorly conidiating mycelium. Suppressing plasmids were recovered from several such transformants and were found to represent two different genes (see MATERIALS AND METHODS). One gene had properties of a transcription factor and will be described elsewhere. The second gene

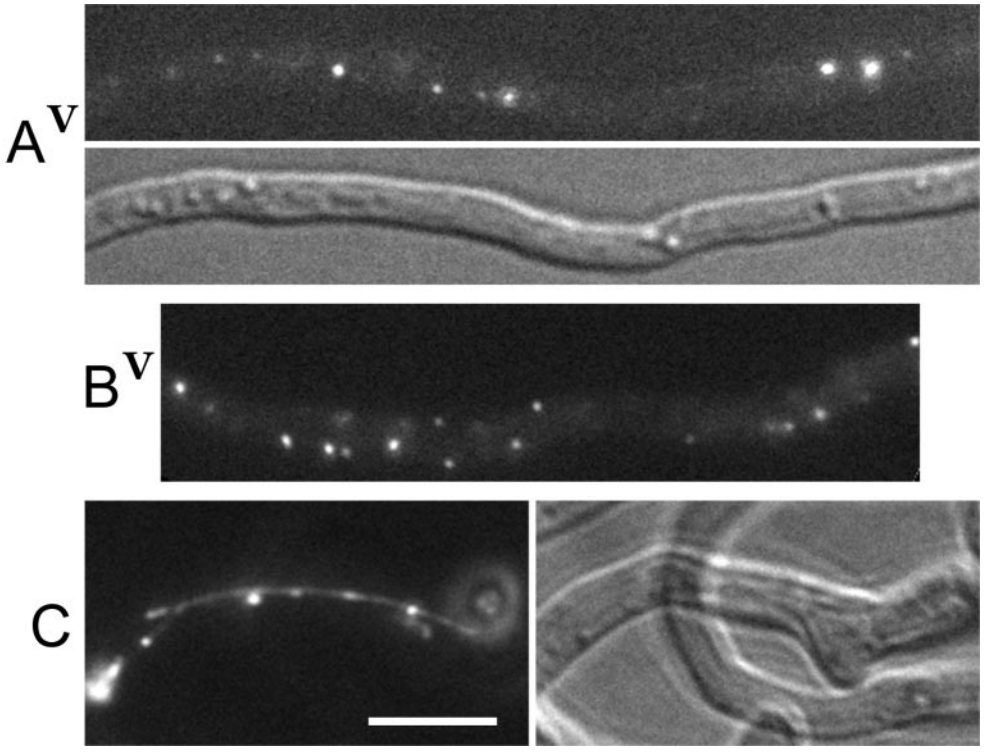

Figure 5. Specks of the GFP-tagged full-length NUDE as observed after integration of several copies of the *alcA(p)::GFP*::nudE* gene at the *nudE* locus. The intensities of images and time-lapse series were adjusted for reproduction purposes. As a result, very bright specks show as round objects instead of sharp dots. (A) Cells were grown in liquid M-glycerol medium for 2 d at 28°C. Ethanol was added to 1.7% (vol/vol) and the image and time series were taken 5 h later. Differential interference contrast image is shown below. The video shows that the specks move in a jerky way and in all directions. (B) Cells were grown as described in A. Benomyl was added to 4 μg/ml together with ethanol, and the image and time series were taken 4 h later. The video shows almost complete lack of movements. (C) In old hyphae, the specks are often imbedded into cables. The cells were grown for 2 d at 26°C on an agar pad of M-glycerol plus ethanol. The image was taken from the crowded area inside the colony. The movements in such areas were rare and were limited to isolated specks outside the cables. Differential interference contrast image is shown to the right. Bar, 5 μm.

turned out to be the *nudF* gene. The suppressor plasmid pAid::*nudF* recovered from one of the transformants carried a ~10-kb genomic DNA fragment with the *nudF* gene (1.3 kb) and no evidence of the *nudE* sequence. A much smaller, ~2-kb genomic DNA fragment with the *nudF* gene also suppressed the *nudE* deletion when cotransformed with pAid. The plasmid pAid::*nudF6*, which carries genomic DNA fragment with a ts allele of the *nudF* gene, suppressed the *nudE* deletion only partially and only at 32°C (our unpublished data).

Remarkably, suppression of the *nudE* deletion by pAid::*nudF* was total (Figure 6A): the Δ*nudE*[pAid::*nudF*] transformants were indistinguishable from the Δ*nudE*[pAid::*nudE*] wild-type control transformants under all conditions tested (YAG and YAGK at 32–43°C, M-glucose at 37°C). The radial growth rates were 14.5 ± 0.2 mm/d for both transformants vs. 9.2 ± 0.2 mm/d for the Δ*nudE*[pAid] control (37°C, YAG). The defects in conidia production mentioned above were also corrected. The NUDF protein level seemed to be unaffected by the deletion of the *nudE* gene (Figure 6B). The NUDF protein level increased ~10-fold after transformation with pAid::*nudF*, consistent with the copy number of ~10 per haploid genome for the *A. nidulans* autonomously replicating vector (Gems *et al.*, 1991).

The pAid::*nudF* plasmid suppressed the ts *nudC3* mutation (Figure 7A). This was expected because the *nudF* gene was isolated as a multicopy suppressor of the *nudC3* mutation during cloning of the *nudC* gene (Xiang *et al.*, 1995a). Suppression was not complete, even under the most permissive conditions for the *nudC3* mutation. As reported previously (Efimov and Morris, 2000), multiple copies of the ts mutant allele of the *nudF* gene, *nudF6*, inhibited the *nudC3* mutant (Figure 7A). In an attempt to identify other *nudC*-interacting genes, a screen for multicopy suppressors of the *nudC3* mutations was conducted using genomic DNA fragments from the *nudF6* mutant to prevent isolation of the *nudF* gene. The screen did not produce any new genes except for the transcription factor-like gene mentioned above (see MATERIALS AND METHODS). Interestingly, several plasmids with a truncated *nudC* gene were isolated. They suppressed the *nudC3* mutation more strongly than pAid::*nudF*, so that the only difference from the wild-type was a slightly reduced conidiation under the most restrictive conditions (43°C, YAG). Sequencing of one such plasmid, pAid::*nudC*Δ, showed that the insert terminates within the last *nudC* intron, resulting in the loss of 10 aa from the NUDC's C terminus.

Considering the diversity of genetic interaction discovered through the multicopy suppressor screens so far, it seemed promising to examine the effects of multicopy plasmids with the *nudF* and other genes using direct transformations of different dynein-related mutants. This approach revealed several new interactions described below. Figure 8 summarizes the effects of multicopy plasmids described herein and in Efimov and Morris (2000).

Multiple Copies of nudF Gene Inhibit a Dynein Heavy Chain Mutant in an Allele-specific Manner

pAid::*nudF* strongly inhibited the ts *nudA1* (cytoplasmic dynein heavy chain) mutant (Figure 7B), whereas pAid::*nudF6*

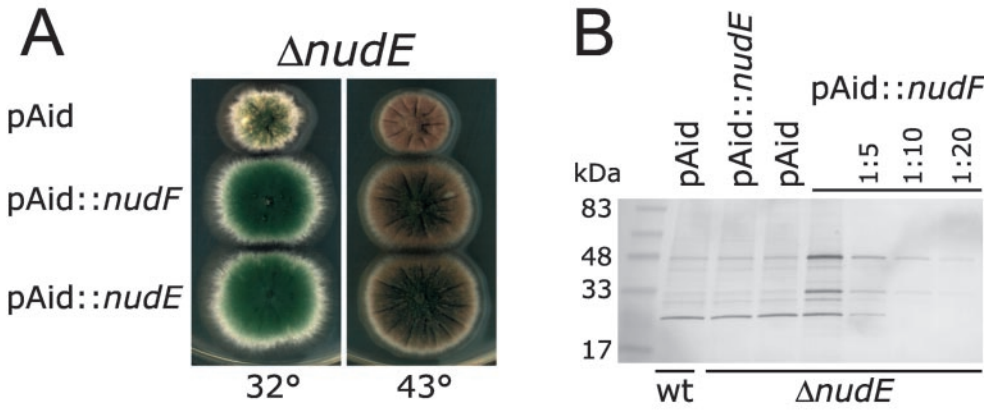

Figure 6. (A) Total suppression of the *nudE* gene deletion by multiple copies of the *nudF* gene. A strain with the deleted *nudE* gene (SF2-9-9) was transformed with the *nudF* and *nudE* genes in the multicopy vector pAid and with the empty vector. Transformants were grown on complete medium (YAG) for 3 d. The strain produces conidia of wild-type color (dark green). (B) NUDF protein level is not affected by the deletion of the *nudE* gene and increases ~10-fold after transformation with the pAid::*nudF* plasmid. Total protein extracts were made from the transformants shown in A as well as from a wild-type strain (GR5) transformed with pAid. Proteins were separated on a 4–20% SDS-PAGE and immunoblotted with an anti-NUDF antibody. Equal amounts (3.3 μg) of protein were loaded in the first four lanes, followed by serial dilutions of the Δ*nudE*[pAid::*nudF*] extract. The uppermost band is the full-length NUDF protein (49 kDa). The ~30-kDa band enriched in the NUDF-overexpressing extract is a NUDF breakdown product. The lowest band is nonspecific and demonstrates equal loading.

had no effect. Neither pAid::*nudF* nor pAid::*nudF6* had any effect on three other ts *nudA* mutants (*nudA2*, *nudA4*, and *nudA5*), on a dynein IC ts mutant (*nudI416*), on a dynactin Arp1 ts mutant (*nudK317*), or on a wild-type strain. Under conditions when inhibition was the strongest (32°C, YAG; Figure 7B), the *nudA1*[pAid::*nudF*] colonies had a typical *nud* phenotype. Examination of nuclear distribution in germlings by DAPI staining showed a more prominent nuclear migration defect compared with the control (our unpublished data). Thus, the growth inhibition most likely resulted from the inhibition of the cytoplasmic dynein and dynactin pathway.

Genetic Interactions between nudF and apsA Genes

The *A. nidulans apsA* and *apsB* mutants were included in the analysis because they display nuclear distribution defects that resemble those in the dynein and *nudF* mutants, although the defects are much less severe (Clutterbuck, 1994; Fischer and Timberlake, 1995; Suelmann *et al.*, 1998; Graïa *et al.*, 2000). In addition, the *S. cerevisiae* homolog of *apsA*, *NUM1*, functions in the cytoplasmic dynein pathway (Geiser *et al.*, 1997; Heil-Chapdelaine *et al.*, 2000; Farkasovsky and Küntzel, 2001). The *apsA1* and *apsA5* mutants were noticeably inhibited by pAid::*nudF* (Figures 7C). Again, pAid::*nudF6* had no effect. The phenotypes of the *apsA1* and *apsA5* mutants were not affected by the growth conditions, and their inhibition by pAid::*nudF* was independent of the temperature or growth medium. The colony radial growth rates of the *apsA1* and *apsA5* mutants bearing pAid::*nudF* were reduced by 22% compared with those of the same strains bearing the empty vector pAid (to 9.7 and 11.1 mm/d from 12.4 and 14.3 mm/d, respectively; 37°C, YAG; SE was <0.4 mm/d).

The third *apsA* mutant analyzed was a Δ*apsA* strain in which 96% of the *apsA* coding region had been deleted (Fischer and Timberlake, 1995). The genotype of this strain precluded the use of pAid-derived plasmids. The Δ*apsA* strain was transformed with the pAid2-derived multicopy plasmids, which carry the *argB* gene instead of the *pyrG* gene as a selective marker. For this reason, the transformants could be analyzed only on minimal media. Complicating the analysis, the Δ*apsA*[pAid2] transformants grew at a slower rate than the wild-type control transformants Δ*apsA*[pAid2::*apsA*] (13.1 vs. 14.7 mm/d; M-glucose, 37°C; SE <0.4 mm/d), whereas the untransformed Δ*apsA* strain grew at the wild-type rate both on complete and minimal media supplemented with arginine. This could indicate that the empty vector pAid2 has an inhibitory effect, or is less efficient in complementing the *argB* mutation in the Δ*apsA* strain than its clones. Such differences between the transformed and untransformed strains were not observed with the pAid vector: strains transformed with pAid, including *apsA1* and *apsA5* mutants, grew at the same or marginally higher rates than the untransformed strains. Nevertheless, the colony radial growth rates of the Δ*apsA*[pAid2::*nudF*] transformants were reduced by 10% compared with those of the Δ*apsA*-[pAid2] controls (11.8 vs. 13.1 mm/d; average for eight transformants each; M-glucose, 37°C; SE <0.4 mm/d). Similar inhibition was observed at 32, 37, and 43°C.

Given the effects of multiple copies of the *nudF* gene on the *apsA* mutants, it was interesting to examine whether there were any mutants affected by multiple copies of the *apsA* gene. pAid::*apsA* had a slight inhibitory effect on the mutants *nudF6* and *nudK317* (our unpublished data) and a more pronounced inhibitory effect on the *nudC3* mutant (Figure 7D). The inhibition of the *nudC3* mutant occurred under conditions partially restrictive for the *nudC3* mutation (37°C, YAG; 43°C, YAGK). No effect could be observed at 32°C when, judging from the smallness of the improvement conferred by pAid::*nudF*, the NUDF protein function was largely normal. In contrast, inhibition by pAid::*nudF6* was noticeable under all conditions, including 32°C. Also, it is clear from the magnitude of the *nudC3* suppression by pAid::*nudF* at 43°C (Figure 7A) that most of the growth defects seen in the *nudC3* mutant are due to the NUDF

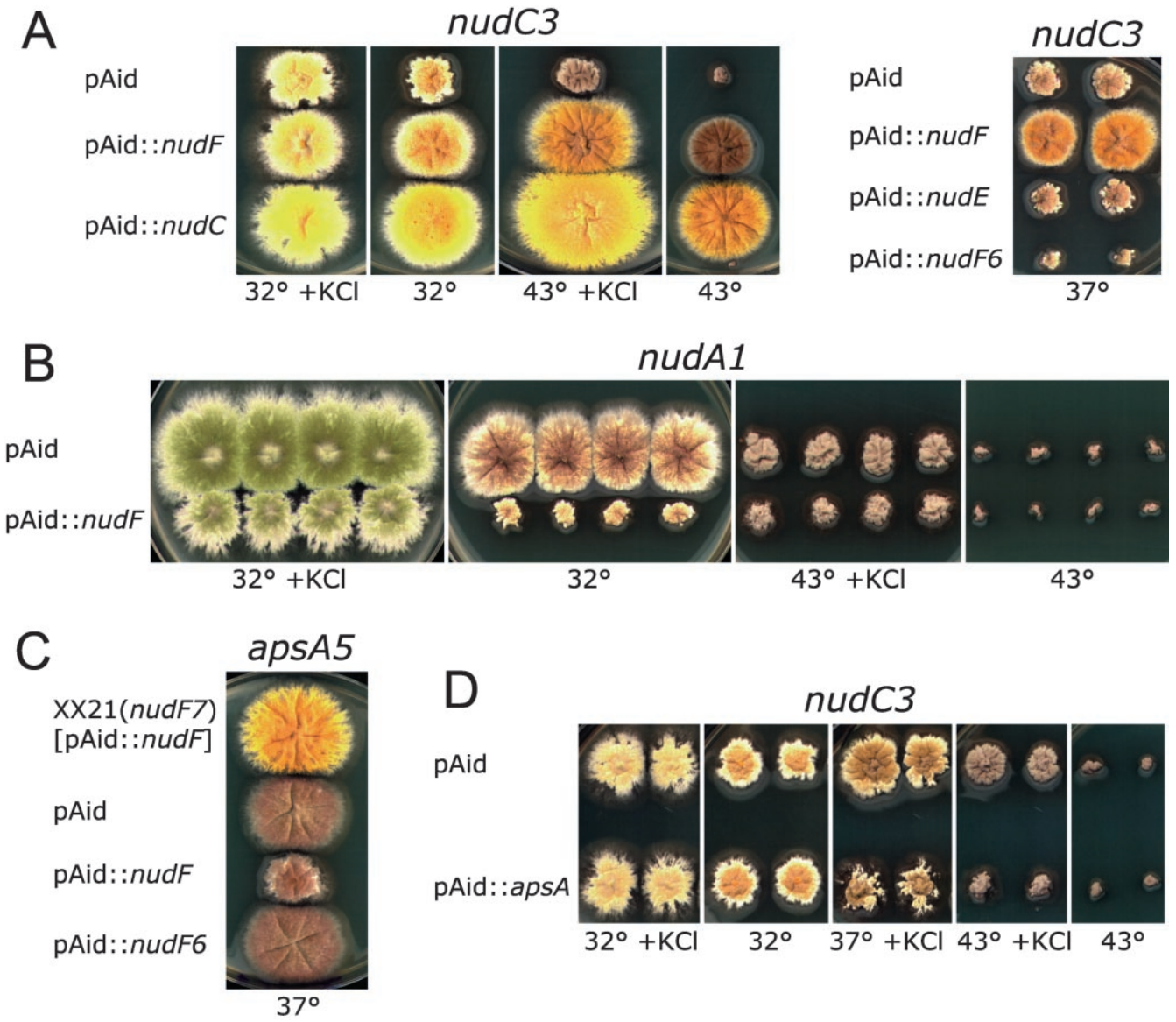

Figure 7. Interactions between the *nudF* gene and *nudC*, *nudA*, *apsA* genes. Shown are *A. nidulans* mutants transformed with multicopy plasmids and grown for 3 d on plates with YAG or YAG plus 0.6 M KCl. The color of conidia is bright green in the *nudA1* strain and yellow in other strains. (A) pAid::*nudF* suppresses the ts *nudC3* mutant (strains C3y-3), whereas pAid::*nudF6* inhibits it. (B) pAid::*nudF* inhibits the ts *nudA1* mutant (strain XX3). (C) pAid::*nudF* inhibits the *apsA5* mutant (strain apsA5). The strain is not affected by the temperature or KCl, and transformants look the same under all conditions. The *apsA1* transformants also looked the same. The top colony is a wild-type control and is the *nudF7* mutant (strain XX21) transformed with pAid::*nudF*. (D) Multiple copies of the *apsA* gene inhibit the ts *nudC3* mutant (strains C3y-3) under partially restrictive conditions.

protein defect. Thus, the inhibitory effect of pAid::*apsA* on the *nudC3* mutant could be due to an *apsA-nudF* interaction rather than an *apsA-nudC* interaction.

Mutations in the *apsA* and *apsB* genes of *A. nidulans* result in similar phenotypes (Clutterbuck, 1994; Fischer and Timberlake, 1995; Suelmann *et al.*, 1998). An *apsB* mutant was transformed with multicopy plasmids and was found to be unaffected by pAid::*nudF* or other plasmids.

Phenotypes of apsA Mutants and Double Mutants apsA5; ΔnudE and apsA5; ΔnudF

The deletion of the *apsA* gene in the Δ*apsA* strain should be a null mutation because it eliminates 96% of the *apsA* coding region (Fischer and Timberlake, 1995). In the *apsA1* allele, the mutation leads to a premature protein termination after aa 1262, thus eliminating the PH domain required for APSA

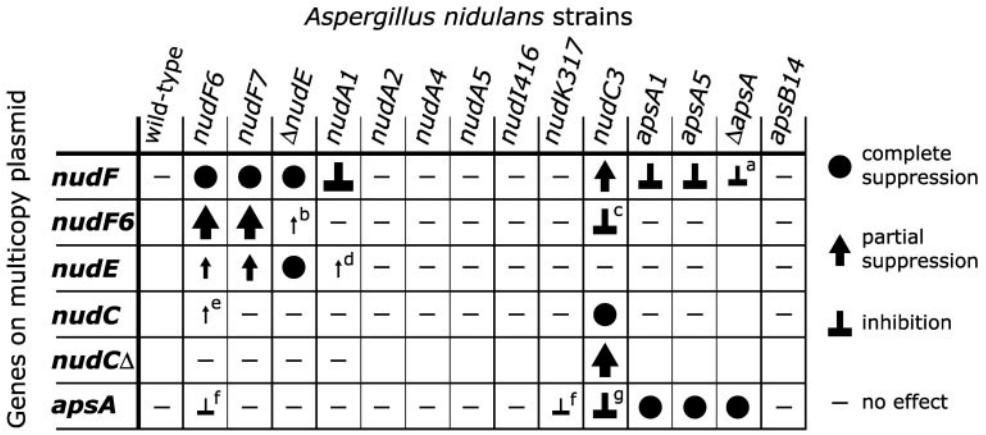

Figure 8. Summary of the effects of multiple copies of different genes on different *A. nidulans* mutants described herein and in the previous work (Efimov and Morris, 2000). The results with the truncated and chimeric *nudE* genes and *GFP*::*nudE* fusions are not shown (Figure 1 in Efimov and Morris, 2000; Figure 3A in this work). That multiple copies of the *nudF* gene suppress the *nudC3* mutation was first reported by Xiang *et al.* (1995a). Each strain was transformed with a multicopy plasmid carrying the indicated gene, and transformants were compared with the same strain transformed with the empty vector. All mutants are conditional (temperature sensitive) except for the *apsA*, *apsB* and deletion mutants. Bigger symbols represent a stronger effect. Untested combinations are left blank. *Notes:* a–multicopy plasmids used to transform SRF30 (Δ*apsA*) strain carry *argB* as a selective marker, while the *pyrG* gene was used as a selective marker for transformation of all other strains; b–the only effect is a slight improvement in conidiation at 32°C, YAG; c–inhibition is observed under all conditions, but is most obvious at 37°C; d–slight improvement in conidiation at 32°C, YAG; e–slight improvement in conidiation at 43°C, YAGK; f–the inhibitory effect is subtle and observed in a narrow range of semirestrictive conditions (43°C, YAGK); g–no effect at 32°C (YAG or YAGK) and at 43°C, YAG, inhibition at 37°C (YAG or YAGK) and at 43°C, YAGK.

targeting to the cell cortex (Suelmann *et al.*, 1997). The nature of the mutation in the *apsA5* allele is not known. It was noticed during the course of this work that the *apsA1* and *apsA5* strains produced slightly smaller colonies than the Δ*apsA* strain. That the *apsA* null mutant grows faster than certain *apsA* mutants has not been reported previously, but the growth rates of several original *apsA* and *apsB* mutants have been reported to vary from 68 to 100% of that of the wild-type (Clutterbuck, 1994). Accurate measurements of colony radial growth rates showed that the Δ*apsA* mutant grew at the wild-type rate, whereas the growth rates of the *apsA1* and *apsA5* mutants were reduced by 15–20%. The latter two mutants grew at the wild-type rate after transformation with pAid::*apsA*, but not with the empty vector pAid, proving that the reduced growth rates were due to the *apsA1* and *apsA5* mutations rather than to background mutations.

To characterize how the defects seen in the *apsA* mutants are related to the *nudE* and *nudF* genes, the *apsA5* mutant was crossed to the Δ*nudE* and Δ*nudF* mutants. The colony radial growth rates of relevant strains are compared in Table 2. The effects of the *apsA5* and Δ*nudE* mutations were additive: the *apsA5;* Δ*nudE* double mutants formed smaller colonies than either of the parents, but still bigger than the Δ*nudF* mutant. Conidiation in the double mutant was also less efficient than in either of the parents. On the other hand, the *apsA5;* Δ*nudF* double mutants were indistinguishable from the Δ*nudF* mutant.

DISCUSSION

Role of NUDE Protein Is Secondary to That of NUDF Protein

The *nudE* gene of *A. nidulans* was isolated as a multicopy suppressor of the *nudF7* ts mutation (Efimov and Morris, 2000; Figure 3A). As it turns out, the *nudF* gene is a multicopy suppressor of a *nudE* mutation (Figure 6). One explanation for these genetic interactions is that NUDE and NUDF share a single function and overexpression of one protein can compensate for the reduced activity of another. However, several observations argue against such interpretation. First, NUDE and NUDF have different domain organization and no sequence similarity. Second, although it is impossible to directly test whether pAid::*nudE* suppresses the Δ*nudF* mutant due to the incompatibility of genetic markers and poor transformation efficiency, circumstantial evidence indicates that multiple copies of the *nudE* gene do not simply bypass the function of the *nudF* gene. As has been reported previously (Figure 1A in Efimov and Morris, 2000), pAid::*nudE* is a much weaker suppressor of the ts *nudF6* mutant than of the less tight ts *nudF7* mutant, even when compared under conditions when both mutants are inhibited to the same extent. The suppression of the *nudF6* mutation is barely detectable under the most repressive conditions (43°C, YAG), when the *nudF6* mutant can serve as a proxy for the *nudF* null mutant. Also, pAid::*nudE* has no effect on the *nudC3* mutant, despite the fact the main defect in the *nudC3* mutant is a reduced NUDF function. These observations make it unlikely that NUDE functions independently of NUDF. In contrast, multiple copies of the *nudF* gene suppress a deletion of the *nudE* gene that should be a null mutation, and most remarkably, the suppression is complete. The suppression is obviously caused by NUDF overexpression, even though the NUDF protein level seems to be unaffected by the *nudE* deletion (Figure 6B). The total suppression of the Δ*nudE* mutation by NUDF overexpression indicates that the only detectable role of the NUDE protein is to assist the function of the NUDF protein.

Certain features of the NUDE protein hint at how it might facilitate the function of NUDF. The N-terminal coiled coil domain of all NUDE homologs is slightly >161 aa, which corresponds to a 24-nm-long coiled coil structure. The LIS1

Table 2. Comparison of growth rates (mm/d)[a] of the *apsA, nudE,* and *nudF* mutants of *A. nidulans*

Wild-type	Δ*apsA*	*apsA1* *apsA5*	Δ*nudE*	*apsA5;* Δ*nudE*	Δ*nudF* *apsA5;* Δ*nudF*
13.1 (GR5) 15.7 (R153)	13.4	10.5	8.5	6.7	3.2

[a] Colony radial growth rates (increase in colony's diameter) were measured at 37°C on YAG medium supplemented with uridine, uracil, arginine, pyridoxine, and *p*-aminobenzoic acid. The standard error of each measurement was less than 0.4 mm/d.

binding part has been mapped roughly to the internal one-third of this coiled coil in the mouse NUDE (Feng *et al.*, 2000). The sequence of the NUDE coiled coil is evolutionarily conserved over its entire length, including the regions upstream and downstream of the LIS1 (and by extrapolation, NUDF) binding region. This suggests that these regions bind other proteins in addition to NUDF/LIS1. Thus, the NUDE coiled coil may serve as a scaffold that facilitates formation of a complex between NUDF and other proteins. It should be noted that mammalian NUDE interacts with many centrosome components and has been proposed to function in centrosome organization (Feng *et al.*, 2000). Because *A. nidulans* NUDE, NUDF, and dynein are not observed at spindle pole bodies, it is not clear whether NUDE has a similar role in fungi. A possible function of LIS1/NUDF is promoting assembly of functional dynein and dynactin complexes, because LIS1 overexpression increases the size of dynein and dynactin complexes and stimulates their retrograde movement (Smith *et al.*, 2000). LIS1 coimmunoprecipitates with both dynein and dynactin and interacts with CDHC and dynactin's subunit dynamitin (Faulkner *et al.*, 2000; Niethammer *et al.*, 2000; Sasaki *et al.*, 2000; Smith *et al.*, 2000; Tai *et al.*, 2002), even though dynein and dynactin are observed as a complex in vitro only under special conditions (Kini and Collins, 2001; Kumar *et al.*, 2001). It is possible that, acting as a scaffold, NUDE coiled coil stabilizes intermediate complexes between NUDF/LIS1 and dynein or dynactin, which ultimately assemble into a fully active motor complex. This could explain why increased NUDF concentration bypasses the requirement for NUDE. The dispensable C-terminal domain of NUDE, which is required for NUDE localization (see below), may have evolved to target the protein more precisely to the sites where dynein, dynactin, and NUDF are assembled, such as microtubule ends.

NUDE Protein Is Targeted by Its C-Terminal Domain to Sites Where NUDF and Dynein Are Concentrated, but That Localization Is Optional for NUDE Function

Previous studies have established that NUDF and dynein/dynactin subunits localize in *A. nidulans* to comet-like structures corresponding to the ends of dynamic cytoplasmic microtubules (Xiang *et al.*, 2000; Han *et al.*, 2001; Zhang *et al.*, 2002). In this work, the same localization was observed with the GFP-tagged NUDE protein. Because NUDE protein binds NUDF/LIS1 and is involved in the cytoplasmic dynein function, it is not surprising that it localizes to the sites where NUDF and dynein/dynactin subunits are concentrated. Paradoxically, the targeting of NUDE to comets is achieved by its C-terminal domain, which is dispensable for the biological activity of NUDE (Efimov and Morris, 2000; Figure 3A). The functional, NUDF-binding N-terminal coiled coil of NUDE does not localize to comets. This indicates that localization to comets is not critical for the NUDE function. However, the NUDE's N-terminal domain is slightly less efficient in complementation assays than the full-length protein, even when expressed from a multicopy plasmid (our unpublished data). It is possible that a permanent localization to the sites where NUDF and dynein are concentrated facilitates the function of NUDE's N-terminal domain. An interesting question is how NUDE-C, which is highly variable in length and sequence among species, is targeted to the comets. NUDE-C may bind CDHC because such interaction has been detected in a two-hybrid system (Sasaki *et al.*, 2000). It is also plausible that NUDE-C has microtubule binding activity because it is serine rich and positively charged: features typical of microtubule binding proteins. Note, however, that mammalian NUDE is concentrated at centrosomes and in axons (Feng *et al.*, 2000; Niethammer *et al.*, 2000; Sasaki *et al.*, 2000), and so far it has not been observed at microtubule ends (Coquelle *et al.*, 2002).

Localization to the ends of dynamic microtubules is common for dynein/dynactin and other microtubule-interacting proteins, but the mechanism and significance of this localization are still under investigation (reviewed by Schroer, 2001; Schuyler and Pellman, 2001; Dujardin and Vallee, 2002). The hierarchy of protein interactions at microtubule ends also remains to be determined. The *A. nidulans* CDHC has been observed in comets in the absence of NUDF (Zhang *et al.*, 2002). This work shows that the CDHC and NUDF proteins do not need the NUDE protein to localize to comets (Figures 1 and 2 and Videos 1 and 2). However, because the *nudE* deletion is completely suppressed by NUDF overexpression, the possibility that NUDE facilitates NUDF localization to comets cannot be ruled out. Even though the functional and NUDF-binding NUDE-N is not seen in comets, it is still possible that it facilitates NUDF targeting to comets by transiently binding both NUDF and a comet's component. It is likely that the interaction between NUDF and NUDE-N is transient. Were it permanent, the NUDE-N would be seen in comets where NUDF is concentrated.

The changes in the behavior of GFP::NUDA comets in the *A. nidulans* Δ*nudE* mutant, observed in this work by using live imaging, mirror the changes in the CDHC and dynactin localization in the *N. crassa* Δ*ro-11* mutant observed by indirect immunofluorescence (Minke *et al.*, 1999). In both cases, the comets (streaks in Minke *et al.*, 1999) were more

prominent and oriented more randomly. In addition, a cloud of diffuse signal around the cluster of comets was frequently observed in this work. A possible cause of these changes is an altered dynamics of microtubules resulting from a compromised dynein/dynactin function (Han *et al.*, 2001). It is also possible that the comets are an accumulation of inactive dynein/dynactin complexes (e.g., on vesicles), which periodically get activated and travel back (Seiler *et al.*, 1999). A compromised dynein activity in the absence of RO11/NUDE would block the retrograde transport and result in a larger accumulation on dynein/dynactin complexes.

Origin of Specks of GFP-tagged NUDE and NUDA Proteins

In still images of hyphae expressing GFP::NUDA or GFP::NUDE the specks show as sharp dots, and it is not obvious that they are different from comets. Live imaging shows that the specks behave very differently in time than comets. Unlike the always unidirectionally moving comets, the specks are either immobile or move in a jerky manner (Videos 2C and 5A). Interestingly, their movement seems to be microtubule dependent because it stops after benomyl treatment (Video 5B). It is likely that the specks are an artifact of protein overexpression. In case of the inducible *GFP::nudA* strains, the specks show only on strongly inducing media. The GFP::NUDA and GFP::NUDE fusions that produce specks never show a bright cytoplasmic fluorescence seen with all other construct that do not produce specks. For instance, hyphae expressing the GFP::NUDE fusion never had such a bright background signal as hyphae expressing GFP::NUDE-N or GFP::NUDE-C (Figure 4). The specks may have the same origin as the "aggresomes" observed in cultured vertebrate cells with certain GFP fusions (Johnston *et al.*, 1998; García-Mata *et al.*, 1999; Wigley *et al.*, 1999; reviewed by García-Mata *et al.*, 2002). If the specks are indeed an artifact of protein overexpression, they will be (and, perhaps, have been) observed with other GFP fusions overexpressed in *A. nidulans*. However, without live imaging, it may be difficult to recognize them because they show simply as dots.

Genetic Interactions among Nuclear Distribution Genes Revealed by the Use of Multiple Gene Copies

The experiments with multicopy plasmids have revealed a number of interactions among the nuclear distribution genes of *A. nidulans* (Figure 8). They are seen as either suppression or inhibition of different mutants by multiple copies of the *nudE*, *nudF*, *nudF6*, *nudC*, and *apsA* genes. Despite the diversity of interactions, some generalizations can be made. First, the majority of them involve the *nudF* gene. The two interactions that do not involve the *nudF* gene (*nudA1* suppression by pAid::*nudE*, *nudK317* inhibition by pAid::*apsA*) are among the weakest. The inhibitory effect of pAid::*apsA* on the *nudC3* mutant could stem from an *apsA-nudF* interaction because the major defect in the *nudC3* mutant is a compromised NUDF function. Second, of four *nudF*-interacting genes (*nudA*, *nudC*, *nudE*, and *apsA*), three (*nudA*, *nudC*, and *nudE*) encode for proteins that are known to bind NUDF/LIS1 (see INTRODUCTION). The relation between the *nudE* and *nudF* genes is discussed above. The strong suppression of the *nudC3* mutant by pAid::*nudF* is explained by reduced levels of the NUDF protein in the *nudC3* mutant (Xiang *et al.*, 1995a), although the reason for the reduction is unknown. The *nudC3* mutation does not affect the level of the NUDC protein (Xiang *et al.*, 1995b) and does not cause a total loss of NUDC function (Chiu *et al.*, 1997). The *nudC* and *nudC3* alleles both interact with the *nudF* gene in a yeast two-hybrid system (Efimov, unpublished data). Thus, the inhibitory effect of multiple copies of the *nudF6* allele on the *nudC3* mutant could result from a physical interaction between the two mutant proteins and from interference of such interaction with NUDC activities. Interestingly, the NUDE and NUDC proteins seem to bind different parts of NUDF, because a mutant NUDF variant unable to dimerize (Ahn and Morris, 2001) still interacts with NUDC, but not with NUDE in a two-hybrid system (Efimov and Ahn, unpublished data).

The strong inhibition of the *nudA1* mutant, but not of three other ts *nudA* mutants, by multiple copies of the *nudF* gene is the first example of an allele-specific interaction between the *nudF* and CDHC genes. The existence of such an allele-specific interaction is consistent with a direct binding of NUDF/LIS1 to CDHC that has been observed in two-hybrid and coexpression/coimmunoprecipitation assays (Sasaki *et al.*, 2000; Tai *et al.*, 2002). An increase in NUDF concentration could result in a more robust formation of a complex between NUDF and the mutant CDHC encoded by the *nudA1* allele. All ts *nudA* mutations used in this study reduce CDHC protein level at restrictive temperatures, and thus are likely to impair CDHC stability or folding (Xiang *et al.*, 1995b). Binding of NUDF to the *nudA1*-encoded mutant protein, especially premature binding, could further destabilize it or trap it in a wrong folding conformation.

The genetic interactions between the *nudF* and *apsA* genes are the first evidence connecting the APSA protein of *A. nidulans* to the cytoplasmic dynein pathway. That APSA might function in the dynein/dynactin pathway is not obvious from the phenotype of *apsA* mutants. Although they display mild nuclear distribution defects (Clutterbuck, 1994; Fischer and Timberlake, 1995), they are much healthier than dynein/dynactin mutants (Table 2). This observation implies that, unlike Num1p, which is required for all dynein functions in yeast (Geiser *et al.*, 1997; Heil-Chapdelaine *et al.*, 2000; Farkasovsky and Küntzel, 2001), APSA is only required for a subset of dynein functions in *A. nidulans*. Consistent with this, the *apsA5;* Δ*nudF* double mutant is identical to the Δ*nudF* mutant. The observed additivity of the *apsA5* and Δ*nudE* mutations does not contradict APSA being in the dynein pathway, because the Δ*nudE* mutation is like a partial loss of the NUDF function, as evidenced by the complete suppression of the Δ*nudE* mutation by NUDF overexpression. Interestingly, the *apsB14* mutation suppresses the Δ*nudF* and Δ*nudA* mutations (Efimov, unpublished data). This and the facts that APSA and APSB localize to different structures and do not coimmunoprecipitate (Suelmann *et al.*, 1998) indicate that APSB functions independently of dynein and APSA, despite the similarity of the *apsA* and *apsB* mutant phenotypes. It is possible that genetic interactions between the *nudF* and *apsA* genes reflect physical interactions among NUDF, APSA, and dynein or dynactin. A biochemical evidence for an association between Num1p and cytoplasmic dynein in *S. cerevisiae* has recently been provided

(Farkasovsky and Küntzel, 2001). Additional experiments are needed to identify the components of dynein or dynactin that bind APSA and the role of NUDF in these interactions. Given APSA localization at the plasma membrane and septa, such interactions would imply dynein presence at the cortex or septa of *A. nidulans*. Although such localization has not been observed so far, association with the ends of dynamic microtubules ideally positions dynein for probing the intracellular space for anchoring factors, perhaps in a manner similar to the capture of vesicles by dynactin associated with the ends of cytoplasmic microtubules in vertebrate cells (Vaughan *et al.*, 2002). Dynein mediated sliding of astral microtubules along the cortex has been observed in *S. cerevisiae* and *Schizosaccharomyces pombe*, but detecting dynein and dynactin at the cortex has proved to be hard to accomplish (reviewed by Dujardin and Vallee, 2002). In *S. pombe*, accumulation of CDHC at sites of contact between the cortex and the ends of astral microtubules that pull the nucleus has been observed (Yamamoto *et al.*, 2001). It will be interesting to see whether the *S. pombe* homolog of APSA/Num1p is the cortical dynein-anchoring factor postulated in the latter work, and whether similar proteins function in higher eukaryotes.

ACKNOWLEDGMENTS

I thank Xin Xiang for providing anti-NUDF antibodies and *A. nidulans* strains, particularly the strains with the GFP-tagged *nudF* and *nudA* genes; Reinhard Fischer for providing *apsA* mutants and plasmids; and N. Ronald Morris for the use of laboratory space and equipment. This work was supported by a Scientist Development Grant from the American Heart Association.

Note added in proof. The *apsA1* and *apsA5* strains grow slower than the *apsA* deletion strain (Table 2) because of the *pyrG89* mutation.

REFERENCES

Ahn, C., and Morris, N.R. (2001). NUDF, a fungal homolog of the human LIS1 protein, functions as a dimer *in vivo*. J. Biol. Chem. *276*, 9903–9909.

Alberti-Segui, C., Dietrich, F., Altmann-Jöhl, R., Hoepfner, D., and Philippsen, P. (2001). Cytoplasmic dynein is required to oppose the force that moves nuclei towards the hyphal tip in the filamentous ascomycete *Ashbya gossypii*. J. Cell Sci. *114*, 975–986.

Aumais, J.P., Tunstead, J.R., McNeil, R.S., Schaar, B.T., McConnell, S.K., Lin, S.H., Clark, G.D., and Yu-Lee, L.Y. (2001). NudC associates with Lis1 and the dynein motor at the leading pole of neurons. J. Neurosci. *21*, 1–7.

Beckwith, S.M., Roghi, C.H., Liu, B., and Ronald, M.N. (1998). The "8-kD"cytoplasmic dynein light chain is required for nuclear migration and for dynein heavy chain localization in *Aspergillus nidulans*. J. Cell Biol. *143*, 1239–1247.

Bruno, K.S., Tinsley, J.H., Minke, P.F., and Plamann, M. (1996). Genetic interactions among cytoplasmic dynein, dynactin, and nuclear distribution mutants of *Neurospora crassa*. Proc. Natl. Acad. Sci. USA *93*, 4775–4780.

Chiu, Y.H., Xiang, X., Dawe, A.L., and Morris, N.R. (1997). Deletion of *nudC*, a nuclear migration gene of *Aspergillus nidulans*, causes morphological and cell wall abnormalities and is lethal. Mol. Biol. Cell *8*, 1735–1749.

Chong, S.S., Pack, S.D., Roschke, A.V., Tanigami, A., Carrozzo, R., Smith, A.C.M., Dobyns, W.B., and Ledbetter, D.H. (1997). A revision of the lissencephaly and Miller-Dieker syndrome critical regions in chromosome 17p13.3. Hum. Mol. Genet. *6*, 147–155.

Clutterbuck, A.J. (1969). A mutational analysis of conidial development in *Aspergillus nidulans*. Genetics *63*, 317–327.

Clutterbuck, A.J. (1994). Mutants of *Aspergillus nidulans* deficient in nuclear migration during hyphal growth and conidiation. Microbiology *140*, 1169–1174.

Coquelle, F.M., *et al*. (2002). LIS1, CLIP-170's key to the dynein/dynactin pathway. Mol. Cell. Biol. *22*, 3089–3102.

Creaser, E.H., Porter, R.L., Britt, K.A., Pateman, J.A., and Doy, C.H. (1985). Purification and preliminary characterization of alcohol dehydrogenase from *Aspergillus nidulans*. Biochem. J. *225*, 449–454.

Dawe, A.L., Caldwell, K.A., Harris, P.M., Morris, N.R., and Caldwell, G.A. (2001). Evolutionarily conserved nuclear migration genes required for early embryonic development in *Caenorhabditis elegans*. Dev. Genes Evol. *211*, 434–441.

Dobyns, W.B., Reiner, O., Carrozzo, R., and Ledbetter, D.H. (1993). Lissencephaly: a human brain malformation associated with deletion of the *LIS1* gene located at chromosome 17p13. J. Am. Med. Assoc. *270*, 2838–2842.

Dujardin, D.L., and Vallee, R.B. (2002). Dynein at the cortex. Curr. Opin. Cell Biol. *14*, 44–49.

Efimov, V.P., and Morris, N.R. (1998). A screen for dynein synthetic lethals in *Aspergillus nidulans* identifies spindle assembly checkpoint genes and other genes involved in mitosis. Genetics *149*, 101–116.

Efimov, V.P., and Morris, N.R. (2000). The LIS1-related NUDF protein of *Aspergillus nidulans* interacts with the coiled-coil domain of the NUDE/RO11 protein. J. Cell Biol. *150*, 681–688.

Farkasovsky, M., and Küntzel, H. (1995). Yeast Num1p associates with the mother cell cortex during S/G2 phase and affects microtubular functions. J. Cell Biol. *131*, 1003–1014.

Farkasovsky, M., and Küntzel, H. (2001). Cortical Num1p interacts with the dynein intermediate chain *Pac*I1p and cytoplasmic microtubules in budding yeast. J. Cell Biol. *152*, 251–262.

Faulkner, N.E., Dujardin, D.L., Tai, C.Y., Vaughan, K.T., O'Connell, C.B., Wang, Y.l., and Vallee, R.B. (2000). A role for the lissencephaly gene *LIS1* in mitosis and cytoplasmic dynein function. Nat. Cell Biol. *2*, 784–791.

Feng, Y., Olson, E.C., Stukenberg, P.T., Flanagan, L.A., Kirschner, M.W., and Walsh, C.A. (2000). LIS1 regulates CNS lamination by interacting with mNudE, a central component of the centrosome. Neuron *28*, 665–679.

Fernández-Ábalos, J.M., Fox, H., Pitt, C., Wells, B., and Doonan, J.H. (1998). Plant-adapted green fluorescent protein is a versatile vital reporter for gene expression, protein localization and mitosis in the filamentous fungus *Aspergillus nidulans*. Mol. Microbiol. *27*, 121–130.

Fischer, R., and Timberlake, W.E. (1995). *Aspergillus nidulans apsA* (anucleate primary sterigmata) encodes a coiled-coil protein required for nuclear positioning and completion of asexual development. J. Cell Biol. *128*, 485–498.

García-Mata, R., Bebök, Z., Sorscher, E.J., and Sztul, E.S. (1999). Characterization and dynamics of aggresome formation by a cytosolic GFP-chimera. J. Cell Biol. *146*, 1239–1254.

García-Mata, R., Gao, Y.S., and Sztul, E. (2002). Hassles with taking out the garbage: aggravating aggresomes. Traffic *3*, 388–396.

Geiser, J.R., Schott, E.J., Kingsbury, T.J., Cole, N.B., Totis, L.J., Bhattacharyya, G., He, L., and Hoyt, M.A. (1997). *Saccharomyces cerevisiae* genes required in the absence of the *CIN8*-encoded spindle motor

act in functionally diverse mitotic pathways. Mol. Biol. Cell *8*, 1035–1050.

Gems, D., Johnstone, I.L., and Clutterbuck, A.J. (1991). An autonomously replicating plasmid transforms *Aspergillus nidulans* at high frequency. Gene *98*, 61–67.

Gems, D.H., and Clutterbuck, A.J. (1993). Co-transformation with autonomously-replicating helper plasmids facilitates gene cloning from an *Aspergillus nidulans* gene library. Curr. Genet. *24*, 520–524.

Graïa, F., Berteaux-Lecellier, V., Zickler, D., and Picard, M. (2000). ami1, an orthologue of the *Aspergillus nidulans apsA* gene, is involved in nuclear migration events throughout the life cycle of *Podospora anserina*. Genetics 155 *633–646*.

Han, G., Liu, B., Zhang, J., Zuo, W., Morris, N.R., and Xiang, X. (2001). The *Aspergillus* cytoplasmic dynein heavy chain and NUDF localize to microtubule ends and affect microtubule dynamics. Curr. Biol. *11*, 719–724.

Heil-Chapdelaine, R.A., Oberle, J.R., and Cooper, J.A. (2000). The cortical protein Num1p is essential for dynein-dependent interactions of microtubules with the cortex. J. Cell Biol. *151*, 1337–1343.

Hirotsune, S., Fleck, M.W., Gambello, M.J., Bix, G.J., Chen, A., Clark, G.D., Ledbetter, D.H., McBain, C.J., and Wynshaw-Boris, A. (1998). Graded reduction of *Pafah1b1* (*Lis1*) activity results in neuronal migration defects and early embryonic lethality. Nat. Genet. *19*, 333–339.

Hoffmann, B., Zuo, W., Liu, A., and Morris, N.R. (2001). The LIS1-related protein NUDF of *Aspergillus nidulans* and its interaction partner NUDE bind directly to specific subunits of dynein and dynactin and to α- and γ-tubulin. J. Biol. Chem. *276*, 38877–38884.

Johnston, J.A., Ward, C.L., and Kopito, R.R. (1998). Aggresomes: a cellular response to misfolded proteins. J. Cell Biol. *143*, 1883–1898.

Kaminskyj, S.G.W. (2001). Fundamentals of growth, storage, genetics and microscopy of *Aspergillus nidulans*. Fungal Genet. Newsl. *48*, 25–31.

Kini, A.R., and Collins, C.A. (2001). Modulation of cytoplasmic dynein ATPase activity by the accessory subunits. Cell Motil. Cytoskeleton *48*, 52–60.

Kitagawa, M., Umezu, M., Aoki, J., Koizumi, H., Arai, H., and Inoue, K. (2000). Direct association of LIS1, the lissencephaly gene product, with a mammalian homologue of a fungal nuclear distribution protein, rNUDE. FEBS Lett. *479*, 57–62.

Kormanec, J., Schaaff-Gerstenschläger, I., Zimmermann, F.K., Perecko, D., and Küntzel, H. (1991). Nuclear migration in *Saccharomyces cerevisiae* is controlled by the highly repetitive 313 kDa NUM1 protein. Mol. Gen. Genet. *230*, 277–287.

Kumar, S., Zhou, Y., and Plamann, M. (2001). Dynactin-membrane interaction is regulated by the C-terminal domains of $p150^{Glued}$. EMBO Rep. *2*, 939–944.

Lee, I.H., Kumar, S., and Plamann, M. (2001). Null mutants of the *Neurospora* actin-related protein 1 pointed-end complex show distinct phenotypes. Mol. Biol. Cell *12*, 2195–2206.

Lei, Y., and Warrior, R. (2000). The *Drosophila Lissencephaly1* (*DLis1*) gene is required for nuclear migration. Dev. Biol. *226*, 57–72.

Liu, Z., Xie, T., and Steward, R. (1999). *Lis1*, the *Drosophila* homolog of a human lissencephaly disease gene, is required for germline cell division and oocyte differentiation. Development *126*, 4477–4488.

Liu, Z., Steward, R., and Luo, L. (2000). *Drosophila Lis1* is required for neuroblast proliferation, dendritic elaboration and axonal transport. Nat. Cell Biol. *2*, 776–783.

Lo Nigro, C., Chong, C.S., Smith, A.C.M., Dobyns, W.B., Carrozzo, R., and Ledbetter, D.H. (1997). Point mutations and an intragenic deletion in *LIS1*, the lissencephaly causative gene in isolated lissencephaly sequence and Miller-Dieker syndrome. Hum. Mol. Genet. *6*, 157–164.

Maruyama, J., Nakajima, H., and Kitamoto, K. (2002). Observation of EGFP-visualized nuclei and distribution of vacuoles in *Aspergillus oryzae arpA* null mutant. FEMS Microbiol. Lett. *206*, 57–61.

Minke, P.F., Lee, I.H., Tinsley, J.H., Bruno, K.S., and Plamann, M. (1999). *Neurospora crassa ro-10* and *ro-11* genes encode novel proteins required for nuclear distribution. Mol. Microbiol. *32*, 1065–1076.

Morris, S.M., Albrecht, U., Reiner, O., Eichele, G., and Yu-Lee, L.-Y. (1998). The lissencephaly gene product Lis1, a protein involved in neuronal migration, interacts with a nuclear movement protein, NudC. Curr. Biol. *8*, 603–606.

Niethammer, M., Smith, D.S., Ayala, R., Peng, J., Ko, J., Lee, M., Morabito, M., and Tsai, L. (2000). NUDEL is a novel Cdk5 substrate that associates with LIS1 and cytoplasmic dynein. Neuron *28*, 697–711.

Osherov, N., and May, G.S. (1998). Optimization of protein extraction from *Aspergillus nidulans* for gel electrophoresis. Fungal Genet. Newsl. *45*, 38–40.

Osmani, S.A., May, G.S., and Morris, N.R. (1987). Regulation of the mRNA levels of *nimA*, a gene required for the G2-M transition in *Aspergillus nidulans*. J. Cell Biol. *104*, 1495–1504.

Osmani, A.H., Osmani, S.A., and Morris, N.R. (1990). The molecular cloning and identification of a gene product specifically required for nuclear movement in *Aspergillus nidulans*. J. Cell Biol. *111*, 543–551.

Plamann, M., Minke, P.F., Tinsley, J.H., and Bruno, K.S. (1994). Cytoplasmic dynein and actin-related protein Arp1 are required for normal nuclear distribution in filamentous fungi. J. Cell Biol. *127*, 139–149.

Reiner, O., Carrozzo, R., Shen, Y., Wehnert, M., Faustinella, F., Dobyns, W.B., Caskey, C.T., and Ledbetter, D.H. (1993). Isolation of a Miller-Dieker lissencephaly gene containing G protein β-subunit-like repeats. Nature *364*, 717–721.

Robb, M.J., Wilson, M.A., and Vierula, P.J. (1995). A fungal actin-related protein involved in nuclear migration. Mol. Gen. Genet. *247*, 583–590.

Sasaki, S., Shionoya, A., Ishida, M., Gambello, M.J., Yingling, J., Wynshaw-Boris, A., and Hirotsune, S. (2000). A LIS1/NUDEL/cytoplasmic dynein heavy chain complex in the developing and adult nervous system. Neuron *28*, 681–696.

Schroer, T.A. (2001). Microtubules don and doff their caps: dynamic attachments at plus and minus ends. Curr. Opin. Cell Biol. *13*, 92–96.

Schuyler, S.C., and Pellman, D. (2001). Microtubule "plus-end-tracking proteins": the end is just the beginning. Cell *105*, 421–424.

Seiler, S., Plamann, M., and Schliwa, M. (1999). Kinesin and dynein mutants provide novel insights into the roles of vesicle traffic during cell morphogenesis in *Neurospora*. Curr. Biol. *9*, 779–785.

Smith, D.S., Niethammer, M., Ayala, R., Zhou, Y., Gambello, M.J., Wynshaw-Boris, A., and Tsai, L.H. (2000). Regulation of cytoplasmic dynein behavior and microtubule organization by mammalian Lis1. Nat. Cell Biol. *2*, 767–775.

Suelmann, R., Sievers, N., and Fischer, R. (1997). Nuclear traffic in fungal hyphae: *in vivo* study of nuclear migration and positioning in *Aspergillus nidulans*. Mol. Microbiol. *25*, 757–769.

Suelmann, R., Sievers, N., Galetzka, D., Robertson, L., Timberlake, W.E., and Fischer, R. (1998). Increased nuclear traffic chaos in hyphae of *Aspergillus nidulans*: molecular characterization of *apsB* and *in vivo* observation of nuclear behavior. Mol. Microbiol. *30*, 831–842.

Swan, A., Nguyen, T., and Suter, B. (1999). *Drosophila Lissencephaly-1* functions with *Bic-D* and dynein in oocyte determination and nuclear positioning. Nat. Cell Biol. *1*, 444–449.

Sweeney, K.J., Prokscha, A., and Eichele, G. (2001). NudE-L, a novel Lis1-interacting protein, belongs to a family of vertebrate coiled-coil proteins. Mech. Dev. *101*, 21–33.

Tai, C.Y., Dujardin, D.L., Faulkner, N.E., and Vallee, R.B. (2002). Role of dynein, dynactin, and CLIP-170 interactions in LIS1 kinetochore function. J. Cell Biol. *156*, 959–968.

Tinsley, J.H., Minke, P.F., Bruno, K.S., and Plamann, M. (1996). $p150^{Glued}$, the largest subunit of the dynactin complex, is nonessential in *Neurospora* but required for nuclear distribution. Mol. Biol. Cell *7*, 731–742.

Vaughan, P.S., Miura, P., Henderson, M., Byrne, B., and Vaughan, K.T. (2002). A role for regulated binding of $p150^{Glued}$ to microtubule plus ends in organelle transport. J. Cell Biol. *158*, 305–319.

Vierula, P.J., and Mais, J.M. (1997). A gene required for nuclear migration in Neurospora crassa codes for a protein with cysteine-rich, LIM/RING-like domains. Mol. Microbiol. *24*, 331–340.

Waring, R.B., May, G.S., and Morris, N.R. (1989). Characterization of an inducible expression system in *Aspergillus nidulans* using *alcA* and tubulin-coding genes. Gene *79*, 119–130.

Wigley, W.C., Fabunmi, R.P., Lee, M.G., Marino, C.R., Muallem, S., DeMartino, G.N., and Thomas, P.J. (1999). Dynamic association of proteasomal machinery with the centrosome. J. Cell Biol. *145*, 481–490.

Willins, D.A., Xiang, X., and Morris, N.R. (1995). An alpha tubulin mutation suppresses nuclear migration mutations in *Aspergillus nidulans*. Genetics *141*, 1287–1298.

Willins, D.A., Liu, B., Xiang, X., and Morris, N.R. (1997). Mutations in the heavy chain of cytoplasmic dynein suppress the *nudF* nuclear migration mutation of *Aspergillus nidulans*. Mol. Gen. Genet. *255*, 194–200.

Xiang, X., Beckwith, S.M., and Morris, N.R. (1994). Cytoplasmic dynein is involved in nuclear migration in *Aspergillus nidulans*. Proc. Natl. Acad. Sci. USA *91*, 2100–2104.

Xiang, X., Osmani, A.H., Osmani, S.A., Xin, M., and Morris, N.R. (1995a). *NudF*, a nuclear migration gene in *Aspergillus nidulans*, is similar to the human *LIS-1* gene required for neuronal migration. Mol. Biol. Cell *6*, 297–310.

Xiang, X., Roghi, C., and Morris, N.R. (1995b). Characterization and localization of the cytoplasmic dynein heavy chain in *Aspergillus nidulans*. Proc. Natl. Acad. Sci. USA *92*, 9890–9894.

Xiang, X., Zuo, W., Efimov, V.P., and Morris, N.R. (1999). Isolation of a new set of *Aspergillus nidulans* mutants defective in nuclear migration. Curr. Genet. *35*, 626–630.

Xiang, X., Han, G., Winkelmann, D.A., Zuo, W., and Morris, N.R. (2000). Dynamics of cytoplasmic dynein in living cells and the effect of a mutation in the dynactin complex actin-related protein Arp1. Curr. Biol. *10*, 603–606.

Yamamoto, A., Tsutsumi, C., Kojima, H., Oiwa, K., and Hiraoka, Y. (2001). Dynamic behavior of microtubules during dynein-dependent nuclear migrations of meiotic prophase in fission yeast. Mol. Biol. Cell *12*, 3933–3946.

Zhang, J., Han, G., and Xiang, X. (2002). Cytoplasmic dynein intermediate chain and heavy chain are dependent upon each other for microtubule end localization in *Aspergillus nidulans*. Mol. Microbiol. *44*, 381–392.